

Progress Report

(For End-Semester Evaluation)



B-Tech Project (CP303)

Development of Sand Composite for High Impact Resistance

Submitted By:

Bommiditha Jyothsnavi (2021MEB1277)

Nishika Nakka (2021MEB1301)

Surkanti Sai Sahasra (2021MEB1328)

Supervised By:

Dr. Srikant Sekhar Padhee

Table of Contents

1. INTRODUCTION.....	3
2. OBJECTIVE	4
3. RECAP of CP302 (Previous Semester)	4
3.1. Materials and Methods:.....	4
3.2. Tests and Results:	4
3.3. Ballistic Testing:	7
3.4 Microstructural Analysis:.....	7
3.5 Conclusion of Previous Semester:.....	7
4. Current Semester Work	8
4.1 DIGIMAT – Displacement Boundary Condition.....	8
4.2 DIGIMAT – Periodic Boundary Condition.....	15
4.3 ABAQUS – Uniaxial Stress Boundary Condition.....	15
4.4 Rule of Mixtures	22
5. Results	22
6. Sieve Analysis	27
7. Contact Angle	28
8. SEM Analysis.....	31
9. 3 Point Bending Test	32
10. Conclusion	41
11. References.....	42

1. INTRODUCTION

As the threat of ballistic impacts continues to rise, the need for solutions that are both effective and economically viable becomes increasingly critical. In response to this challenge, sand-based composites have gained attention for their potential as cost-effective materials offering robust ballistic protection. This ongoing research builds upon our previous work (Development Engineering Project) with sand-reinforced epoxy composites, where we successfully demonstrated the material's potential for high-impact resistance. Now, the project is expanding its focus to further optimize the material's properties and investigate its application in enhancing ballistic impact resistance through both experimental and computational approaches.

The current study explores the integration of sand into polymer matrix composites in a graded manner, designed to provide a stepwise defense against varied ballistic threats. The composite features a dense, brittle, and hard base impact zone, capable of eroding projectiles, followed by a less dense region that enhances tensile strength and reflects tensile waves, reducing overall impact energy. By incorporating sand particles, the composite's surface area increases, leading to better adhesion between the inclusions and the epoxy matrix. This improved adhesion facilitates more efficient load transfer, resulting in greater hardness and enhanced energy dissipation.

In the previous semester, we focused on optimizing the mechanical properties of the composite through experimental methods, using different epoxy formulations and molds to enhance the material's performance. Comprehensive testing—including tensile, Izod impact, and flexural assessments—was conducted to evaluate the mechanical and physical properties of the composites. Initial experimental results showed that adjusting the volume fraction of sand significantly impacts both the mechanical performance and ballistic resistance of the material. These findings highlighted the potential of sand as an environmentally sustainable and cost-effective reinforcement for advanced ballistic protection applications.

This semester, we are taking a more computational approach to further refine our understanding of the material's behavior. While we initially relied on sand properties from existing research papers, we are now focusing on calculating these properties using advanced computational techniques. This includes the application of the Rule of Mixtures, Digimat, and Abaqus to model and simulate the behavior of the composite under various boundary conditions. The insights gained from this semester's work will help us refine the material's performance and move closer to achieving a cost-effective, sustainable solution for ballistic protection.

2. OBJECTIVE

The primary objective of our project is to enhance the impact resistance of polymer matrix composites through the inclusion of sand in a graded manner. By utilizing sand as a reinforcement, the goal is to create a cost-effective and environmentally sustainable composite material capable of offering robust protection against varied ballistic threats. This research aims to optimize the mechanical properties of the composite such as hardness, tensile strength, and energy dissipation by experimenting with different sand types, volume fractions, and epoxy formulations. Ultimately, the project seeks to develop an efficient, economical, and sustainable solution for advanced ballistic protection applications.

3. RECAP of CP302 (Previous Semester)

In the previous semester, we focused on experimental testing of the composite with varied sand sizes and volume fractions. We also worked on creating the ballistic samples.

3.1. Materials and Methods:

3.1.1 Epoxy and Hardener: Initially, ER099 epoxy with EH150 hardener was used. Later, LY556 epoxy with HY951 hardener was introduced for its enhanced toughness, flexibility, and adhesion properties. LY556 epoxy was chosen for its superior mechanical, dynamic, and thermal properties, including high resistance to chemical reactions and acids up to 80°C, low viscosity, and long pot life.

3.1.2 Sand Processing: Construction sand, rich in silica, was processed through drying, cleaning, milling, and sieving to achieve uniform particle sizes (0.15 mm, 0.3 mm, 0.425 mm, and 0.6 mm) for optimal composite performance. The irregular shape of the sand particles improved their adhesion within the epoxy matrix, reducing voids and enhancing structural strength.

3.1.3 Sample Preparation: Samples were prepared by mixing epoxy, hardener, and sand in varying volume fractions. The mixture was poured into 3D-printed molds, cured, and post-processed for testing. The use of 3D-printed molds improved precision and efficiency in sample preparation.

3.2. Tests and Results:

3.2.1 Impact Test: Charpy-Izod impact tests showed that increasing the sand volume fraction generally improved impact strength, with the highest impact resistance observed at 70% sand volume. The tests indicated that sand-reinforced composites could effectively dissipate impact energy, making them suitable for high-impact applications.

S.No	Sample Type	Sample1	Sample2	Sample3	Sample4	Sample5	Average
1	10% Silica + Epoxy	39.2	57.2	42.6	-	-	46.33333333

2	20% Sand - 425 micron	25.8	32.4	8	16.8	-	20.75
3	30% Sand - 425 micron	32.4	33	31	-	-	32.13333333
4	40% Sand - 425 micron	29	49.8	25.8	-	-	34.86666667
5	50% Sand - 425 micron	32.4	29	42.6	52	19.6	35.12
6	60% Sand - 425 micron	42	42.6	55	70	-	52.4
7	70% Sand - 425 micron	93.4	157	29	29	-	77.1
8	20% Silica - 300 micron	68.8	22.8	42.6	53.4	-	46.9
9	30% Sand - 600 micron	35	46.2	52.2	75	-	52.1
10	40% Sand - 600 micron	68.8	49.8	35.8	90	-	61.1
11	50% Sand - 600 micron	45	53.4	60	161.8	-	80.05

3.2.2 Tensile Test: Tensile tests revealed that Young's modulus increased significantly with higher sand volume fractions, with the highest modulus observed at 70% sand volume for 0.6 mm sand particles. This indicated that sand reinforcement could significantly enhance the stiffness of the composite material.

Sand Gradation	Sand Percentage	Young's Modulus			
		1	2	3	Average
0.425	20%	1204.3	1239.9	1186.8	1210.67
	30%	1320.4	1315.9	1308.2	1314.83
	40%	1349.8	1326.5	1327.6	1334.63
	50%	1392.9	1365.9	1388.3	1382.367
	60%	1452.5	1428.3	1576.6	1485.8
	70%	1066	1103.7	1170	1113.233
Pure		1173.1	1193.6	1198.2	1188.3
0.3	20%	1214.3	1197	1199.6	1203.633
	30%	1466.8	1414.2	1459.9	1446.967
	40%	1622.5	1545.6	1614.9	1594.33
	60%	1705.4	1704.1	1545.6	1651.7
	70%	1838	1813.6	1774.4	1808.67
0.6	20%	2123.2	2010.12	2125.27	2086.19
	30%	2766.9	2346.19	2275.12	2462.73

	40%	2801.1	2552.25	2424.45	2592.6
	50%	2935.7	2782.27	2537.57	2751.84
	60%	3041.7	3042.5	3115.2	3066.46
	70%	3257	3157.77	3259.5	3224.75

3.2.3 Flexural Test: Flexural tests indicated that sand reinforcement improved the flexural strength of the composites, with the best performance observed at 40% sand volume. The tests demonstrated that the composites could withstand bending forces effectively, making them suitable for structural applications. The ASTM Standard of the samples is ASTM D790

Sand percentage	Young's Modulus (Mpa)				
	Sample-1	Sample-2	Sample-3	Sample-4	Average
30%	49.1	51.9	49.9	44.9	48.95
40%	59.1	60	60.5	63.5	60.775
60%	21.8	37.6	62.9	49.6	42.975

Yield Stress(Mpa)				
Sample-1	Sample-2	Sample-3	Sample-4	Average
11.5	9.78	12	10.8	11.02
12.1	13.3	12.9	9.12	11.855
1.65	16.7	17.3	13.9	12.3875

Ultimate Stress (Mpa)				
Sample-1	Sample-2	Sample-3	Sample-4	Average
11.48	9.78	12	10.8	11.015
12.09	13.28	12.9	9.12	11.8475
13.5	16.68	17.29	13.89	15.34

3.2.4 Hardness Test: Shore D hardness tests demonstrated that hardness increased with higher sand volume fractions, with the highest hardness observed at 70% sand volume for 0.6 mm sand particles. This indicated that sand reinforcement could significantly enhance the material's resistance to indentation and wear.

Particle Size (μm)	0	20	30	40	50	60	70
300 microns	73.2	77	80.8	82	-	83	82.9
	72	75	81.5	81.9	-	81.6	83
	73.1	74	79.8	80.7	-	82.1	82.7
425 microns	73.2	77.9	79.7	80.7	83.7	86.2	89

	72	77	80.1	80.2	82.2	85.1	88.4
	73.1	74	80.4	80.5	82.7	86.4	89.2
600 microns	73.2	75	76.7	78.4	78.1	86.7	90.5
	72	76.4	77.2	78.7	79.5	89.5	91.9
	73.1	75.8	78.4	78.1	78.9	89.1	95.5

3.3. Ballistic Testing:

Ballistic samples were prepared and tested using an INSAS rifle at different firing distances. The LY556 epoxy samples showed superior impact absorption compared to ER099 epoxy samples, with larger impact areas and better resistance to damage. The tests indicated that the LY556 epoxy, when reinforced with sand, could effectively dissipate impact energy and resist damage from high-velocity projectiles. However, delamination was observed in samples with increased layering, indicating the need for improved bonding techniques between layers. This highlighted the importance of optimizing the interfacial bonding and layering process to enhance the material's structural integrity under high-impact conditions.

3.4 Microstructural Analysis:

Optical microscopy revealed that smaller sand particles and lower volume fractions resulted in fewer agglomerations and voids. Higher sand volume fractions led to denser regions but also increased the risk of agglomeration and localized stress. The analysis indicated that the distribution of sand particles within the epoxy matrix played a crucial role in determining the material's mechanical properties and performance.

3.5 Conclusion of Previous Semester:

The incorporation of sand particles into epoxy resin significantly enhanced the material's mechanical properties, particularly in terms of stiffness and impact resistance. The LY556 epoxy, when reinforced with sand, demonstrated superior ballistic performance compared to ER099 epoxy. The project successfully demonstrated the potential of sand-reinforced epoxy composites for ballistic protection, with significant improvements in impact absorption, stiffness, and hardness. However, challenges such as agglomeration and delamination at higher sand volume fractions and layered structures were identified, indicating areas for future improvement. These challenges highlighted the need for further optimization of the material's composition and manufacturing process to enhance its performance and durability.

4. Current Semester Work

The primary goal for pre-midsem this semester was to determine the properties of sand inclusions through computational modelling and simulation, rather than relying on literature values which we used last semester. This approach allows us to gain a deeper understanding of the material's behaviour and to validate our experimental results with more accurate predictions.

4.1 DIGIMAT – Displacement Boundary Condition

We generated our representative volume element using DIGIMAT and altered the modulus of sand such that we reach the modulus value of the composite which we extracted from our experiment. In this way we will get the property of the sand when the displacement boundary condition is applied.

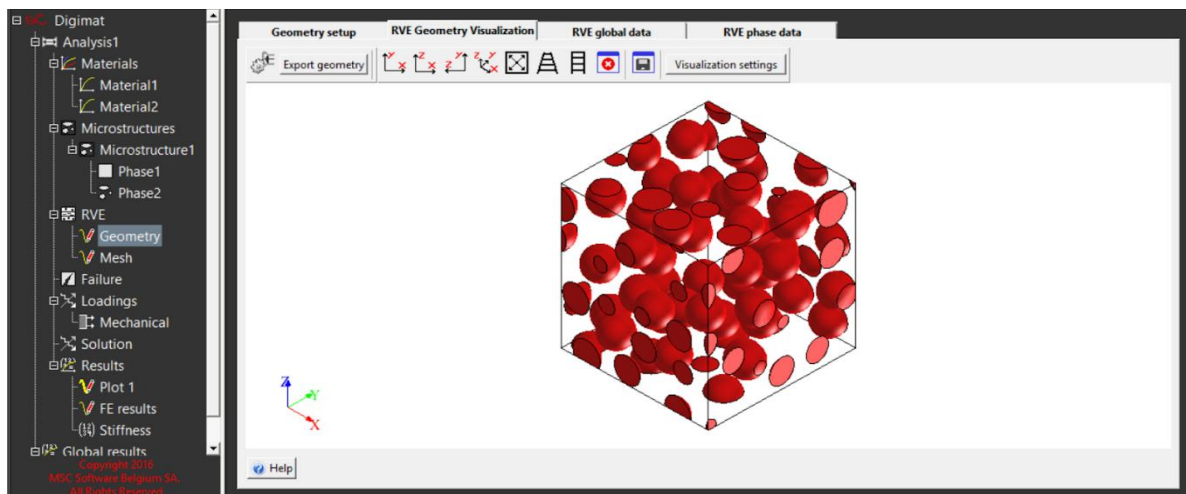
The material property of modulus: E_{epoxy} – 1.18e9 Pa, Density_{epoxy} = 1200kg/m³

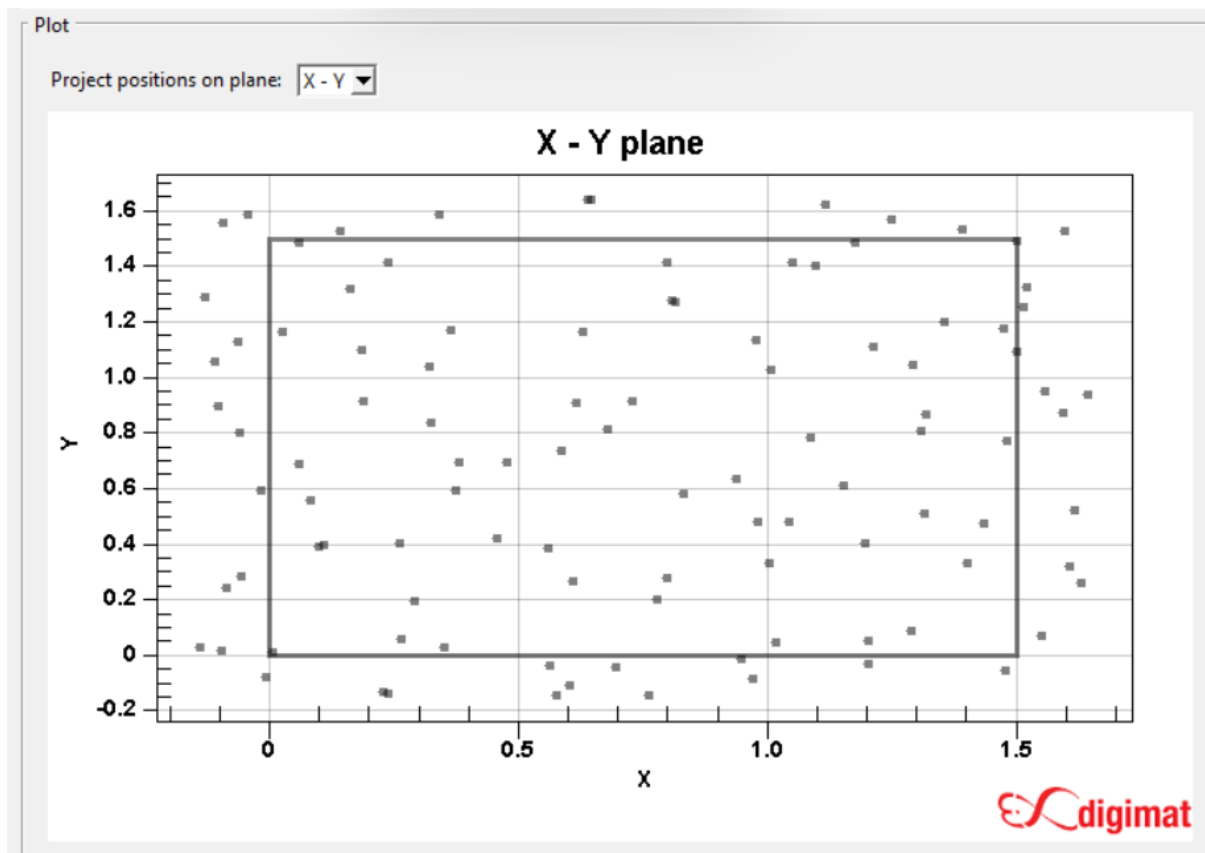
4.1.1 RVE Generation

The images for one sand particle size are shown in the report. Diameter = 0.3mm

The materials were assigned for sand and epoxy and phases were created.

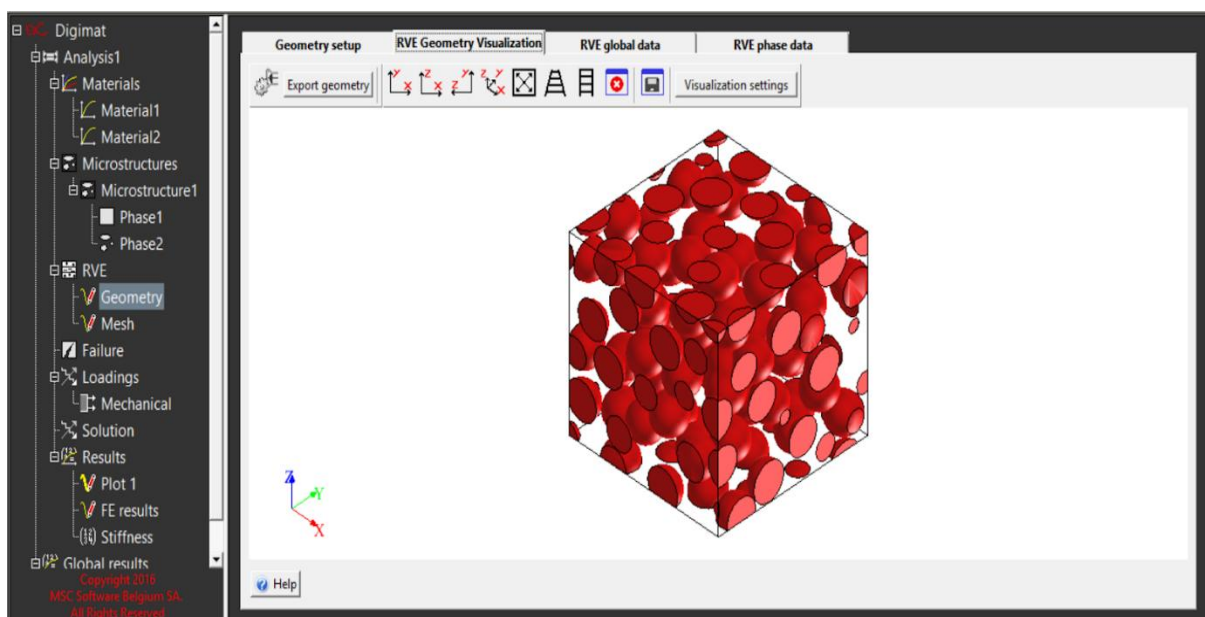
1. 20% Volume Fraction



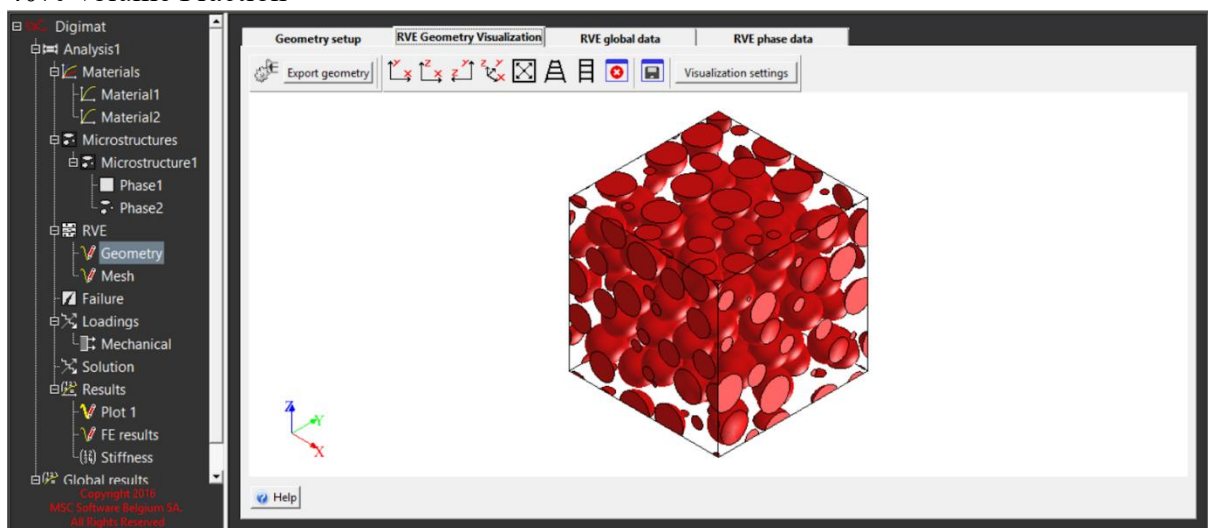


The above graph and the summary data table shows that the distribution of our inclusions is random. The difference between the standard deviations is very less which also supports the randomness of the inclusions.

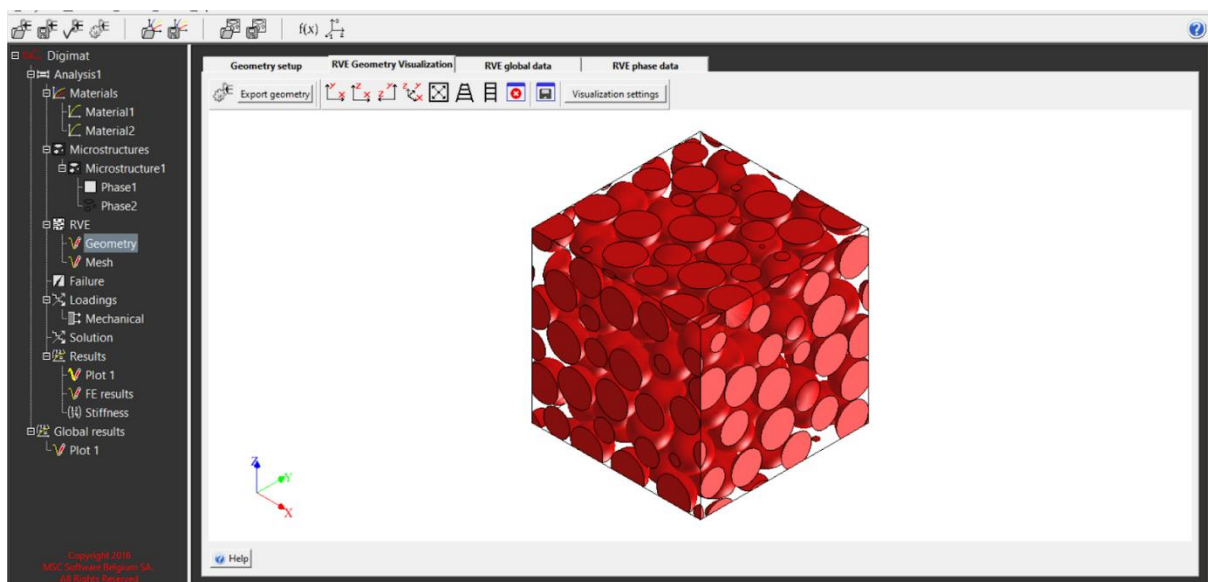
2. 30% Volume Fraction



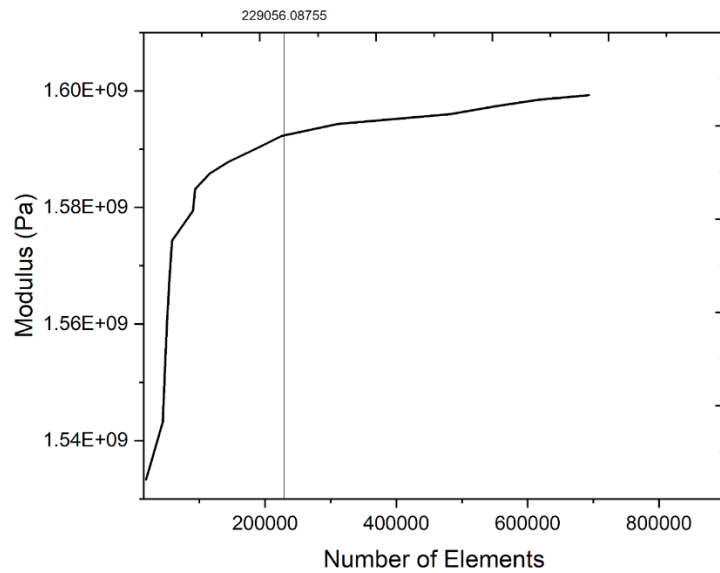
3. 40% Volume Fraction



4. 50% Volume Fraction



5.1.2 Element Size Determination

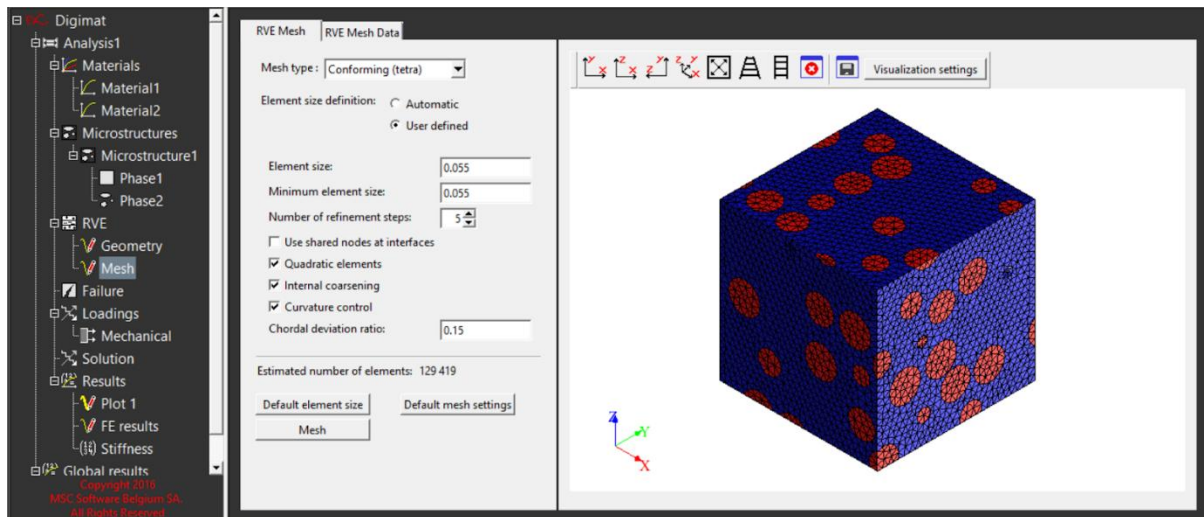


The element size which matches the number of elements in DIGIMAT is 0.055.

4.1.2 Mesh Generation

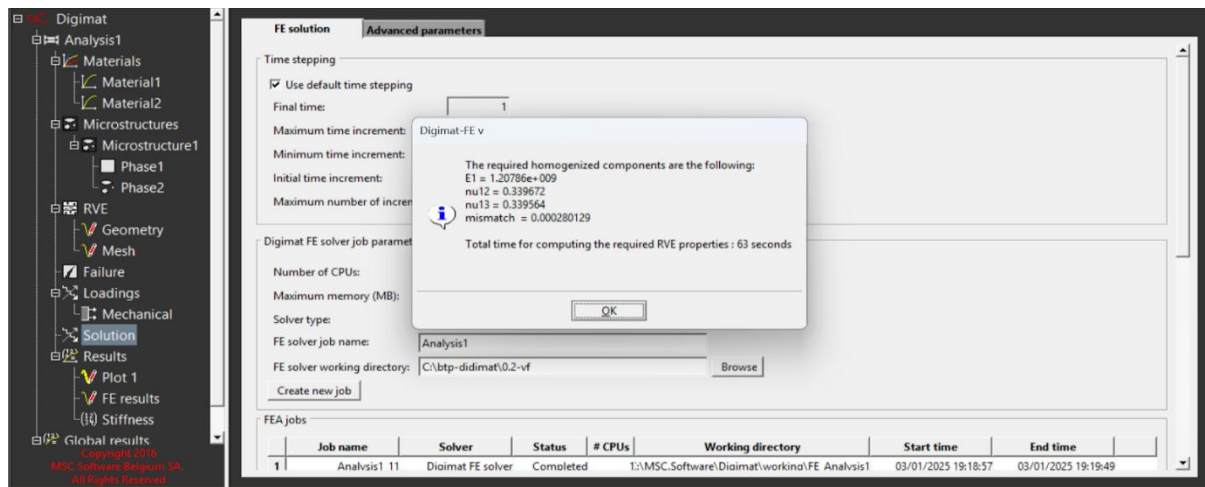
20% Volume Fraction

The element size which we specified here is the one we extracted i.e. 0.055



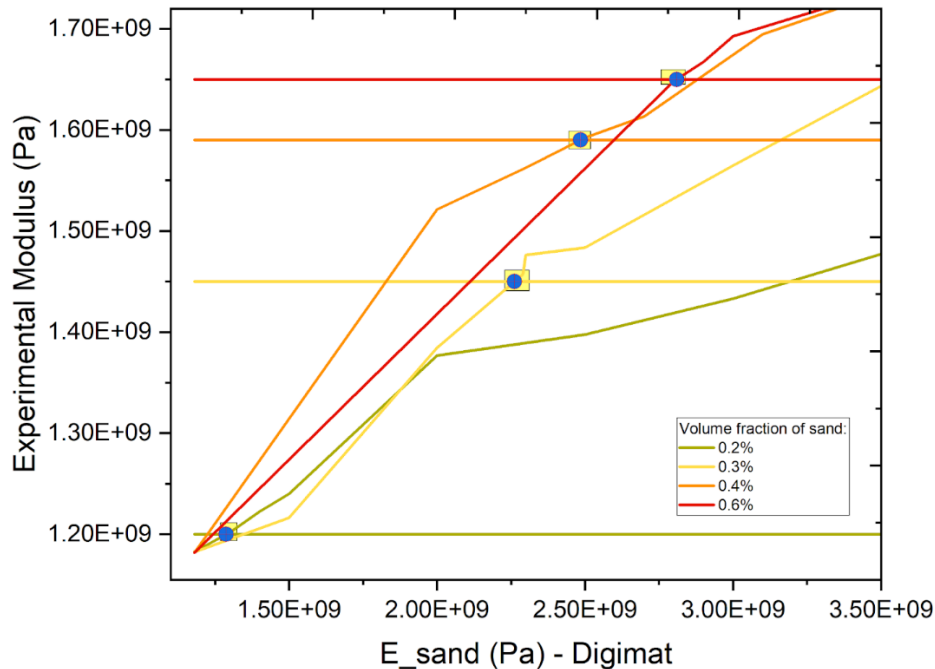
Similarly for all the other sizes and volume fractions mesh can be generated.

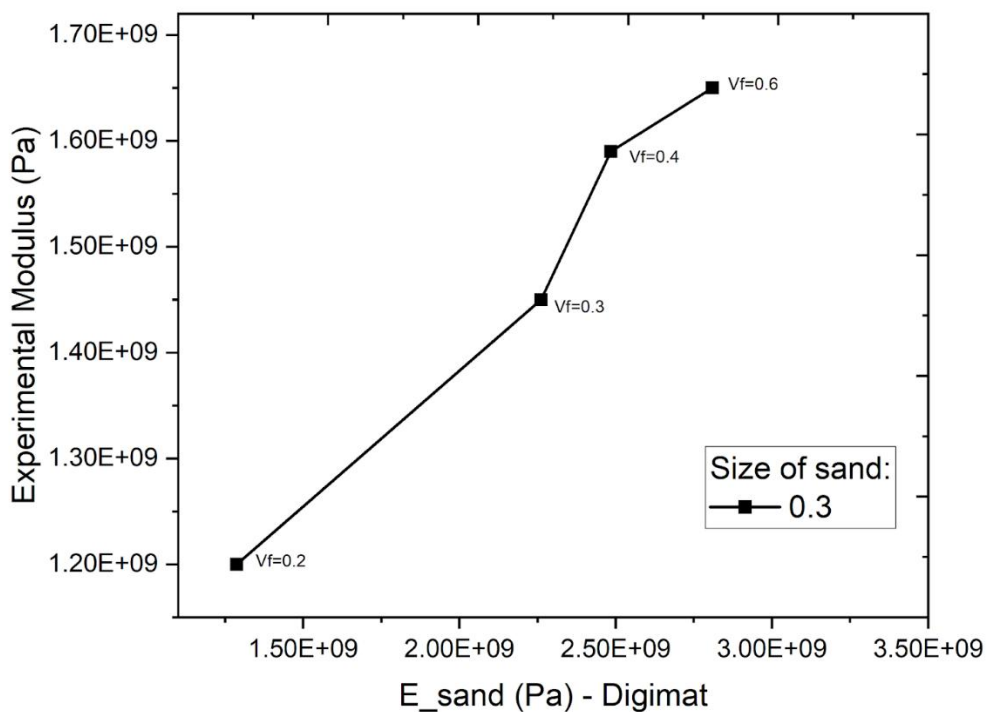
5.1.4 Modulus values



Size of Sand = 0.3mm, 0.2 Vf	E_sand	Effective_Sand (from Digimat)
Modulus = 1203633300	6480000000	1655280000
	50000000000	1602370000
	45000000000	1594040000
	30000000000	1432980000
	15000000000	12400000000
	13000000000	1202070000
	11800000000	1182810000

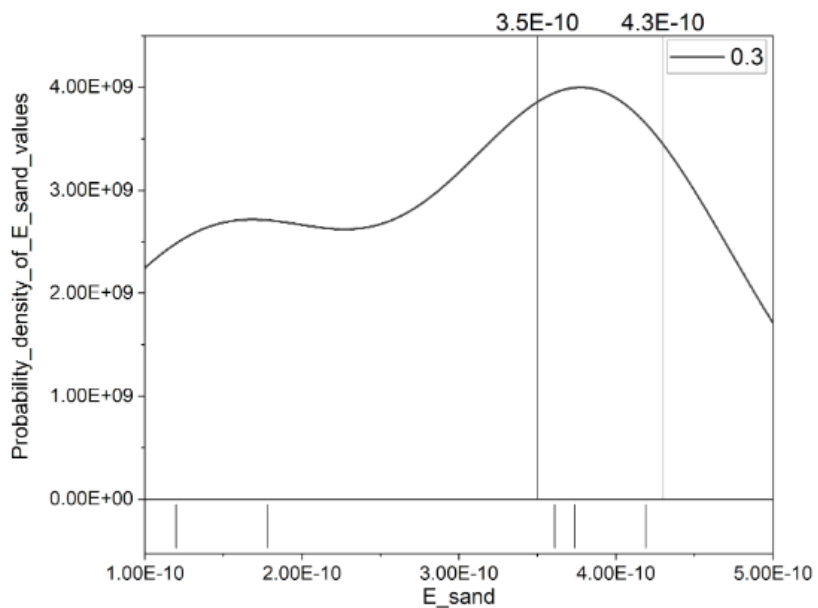
5.1.5 Intersection Graph of Experimental and DIGIMAT values of composite



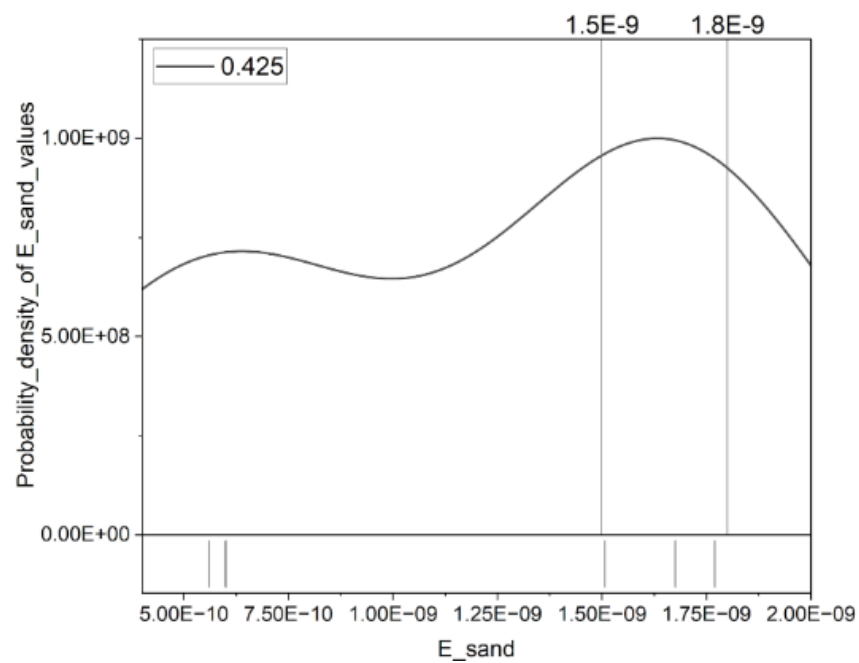


5.1.6 Distribution Graph of Modulus of sand

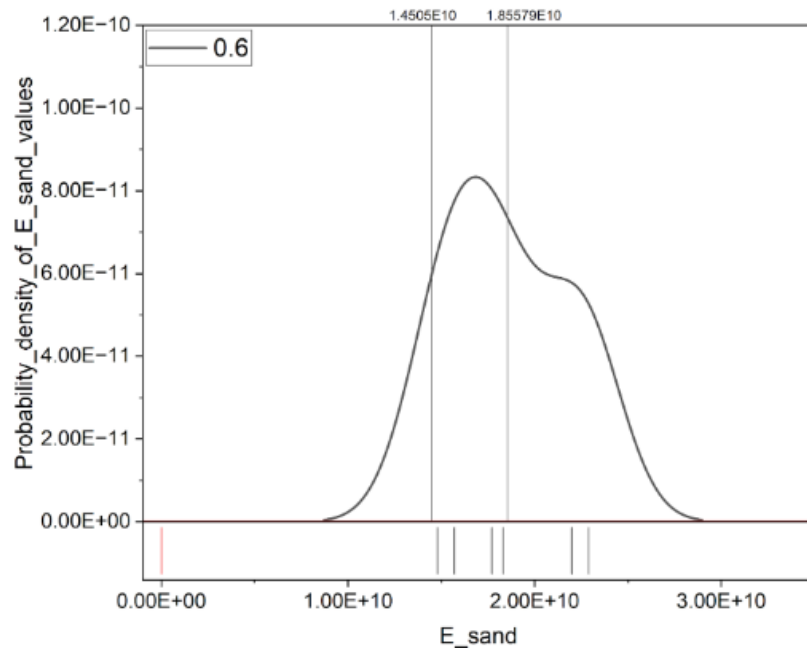
(i) 0.3mm size



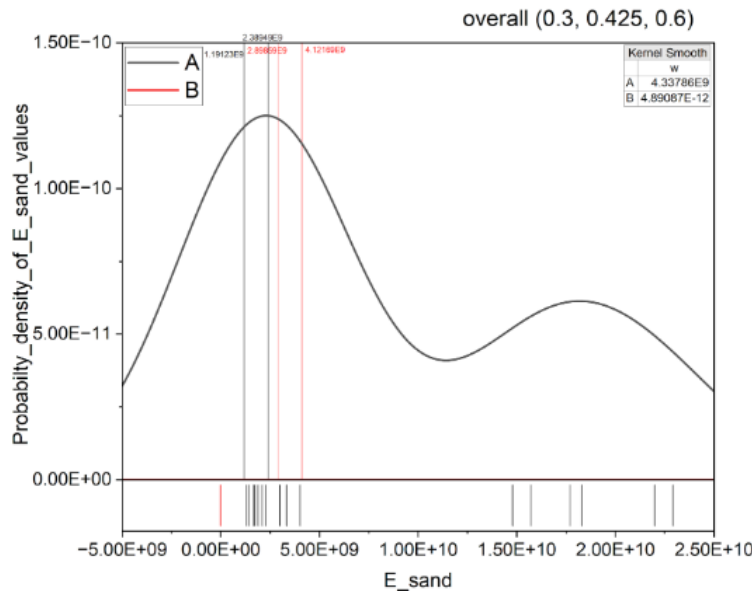
(ii) 0.425mm



(iii) 0.6mm



Overall Range in which our E_sand lies is determined from the combined graph:



4.2 DIGIMAT – Periodic Boundary Condition

We generated our representative volume element using Digimat and altered the modulus of sand such that we reach the modulus value of the composite which we extracted from our experiment. In this way we will get the property of the sand when the composite undergoes periodic boundary condition.

The material property of modulus: E_epoxy – 1.18e9 Pa , Density_epoxy = 1200kg/m³

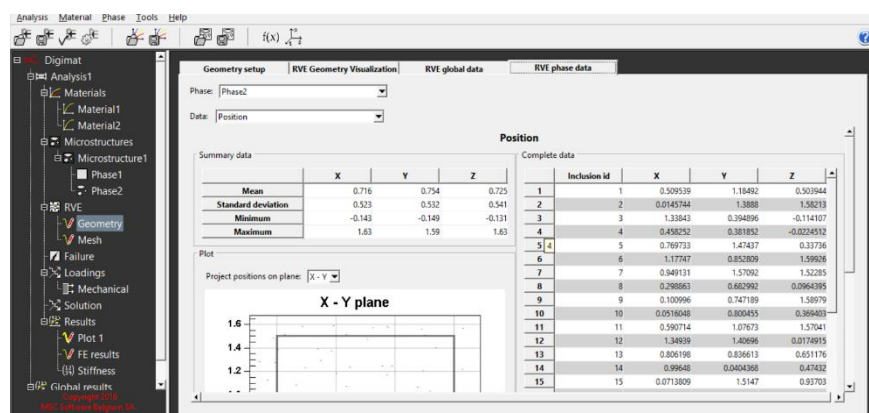
The boundary condition and geometry should be selected as Periodic. Rest of the process remains similar to displacement boundary condition.

4.3 ABAQUS – Uniaxial Stress Boundary Condition

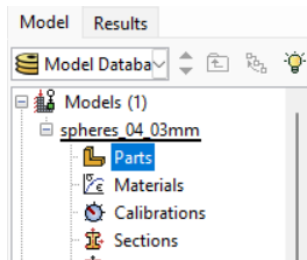
We applied uniaxial stress on our RVE in Abaqus to extract the properties of sand.

Step 1: Creation of Python Script:

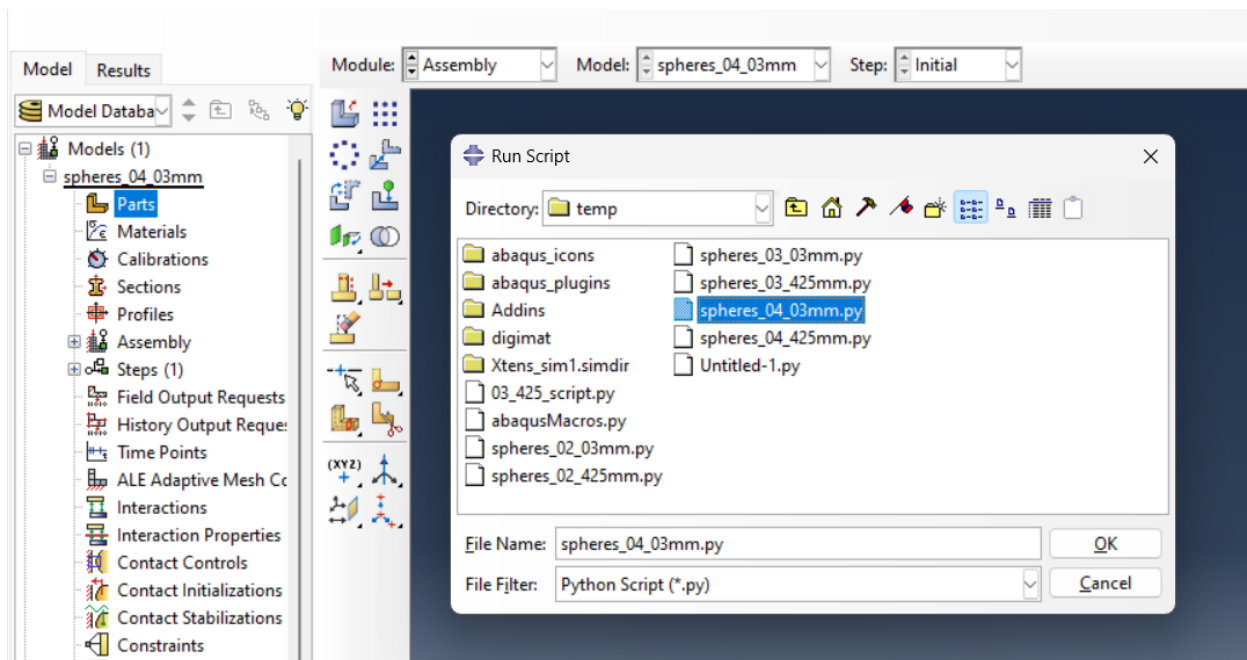
The coordinates of the inclusions of the RVE were taken from DIGIMAT for the respective size and volume fraction and python script is created.



Step 2: Rename the part to the name of the python script: Here it is ‘spheres_04_03mm’

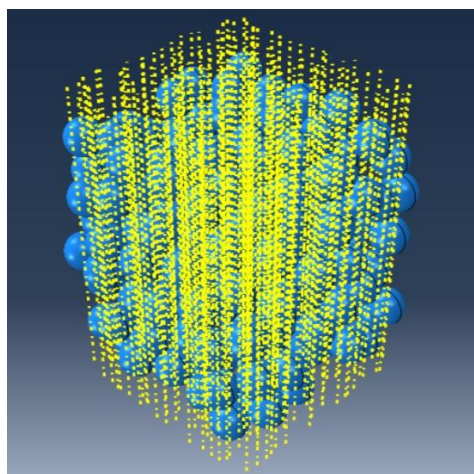


Step 3: Run the python script of inclusions:



The inclusions will be exported after running the file.

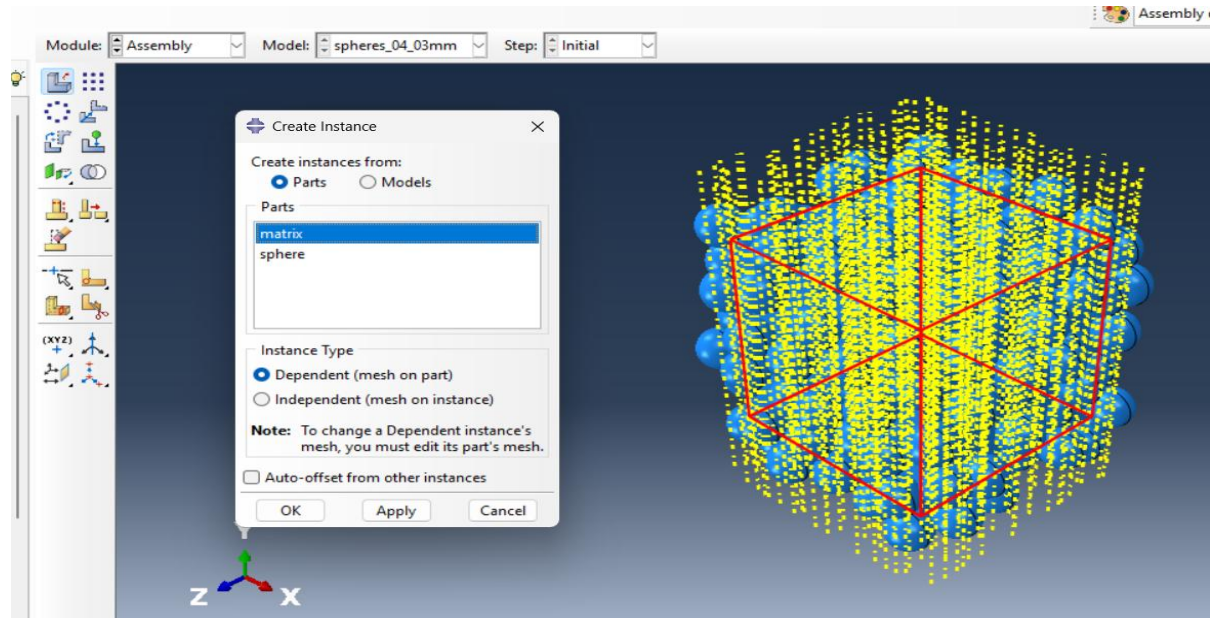
The coordinates of these inclusions were taken from the RVE created in Digimat inorder to ensure similar RVE formation in Abaqus.



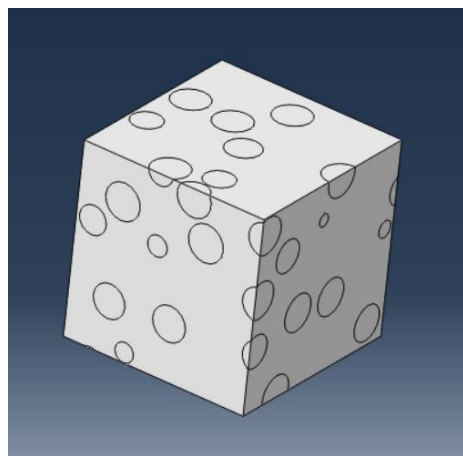
Step 4: Create the Matrix part and Merge with the inclusions:

The size of the matrix should be given as the size of the RVE in Digimat. Here the size is '0.002125 m'.

Then merge both inclusions and matrix part in order to form the composite part

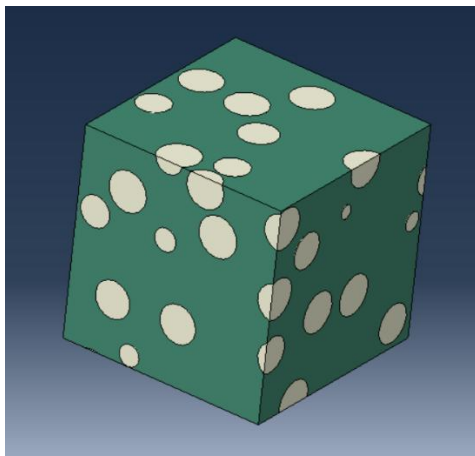


The RVE formed is as follows:

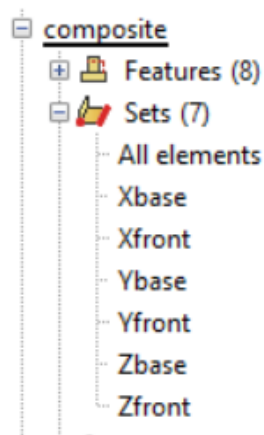
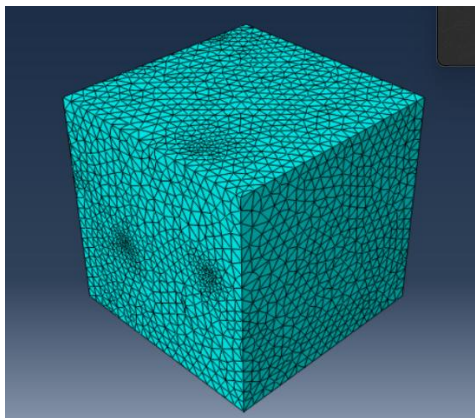


Step 5: Assign Material Properties:

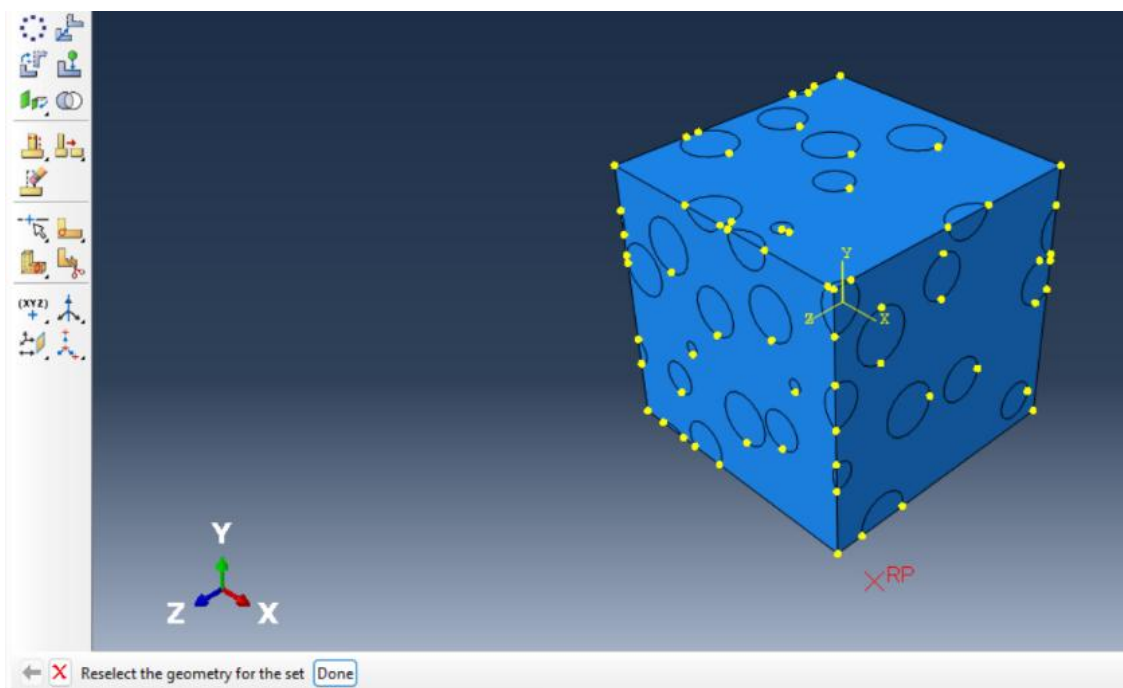
The material property of the epoxy is the same as before. The sand properties are varied and checked in order to get a final composite value which matches our experimental value. The composite after the materials are assigned looks as follows.



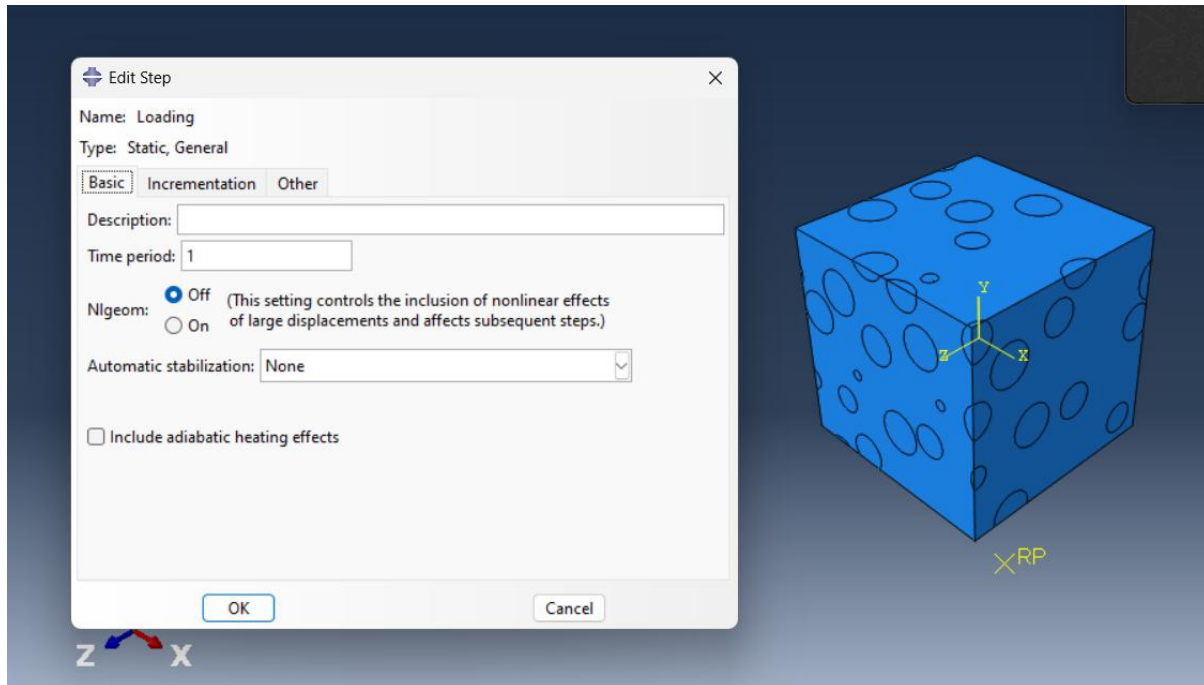
Step 5: Mesh the composite and create the sets:



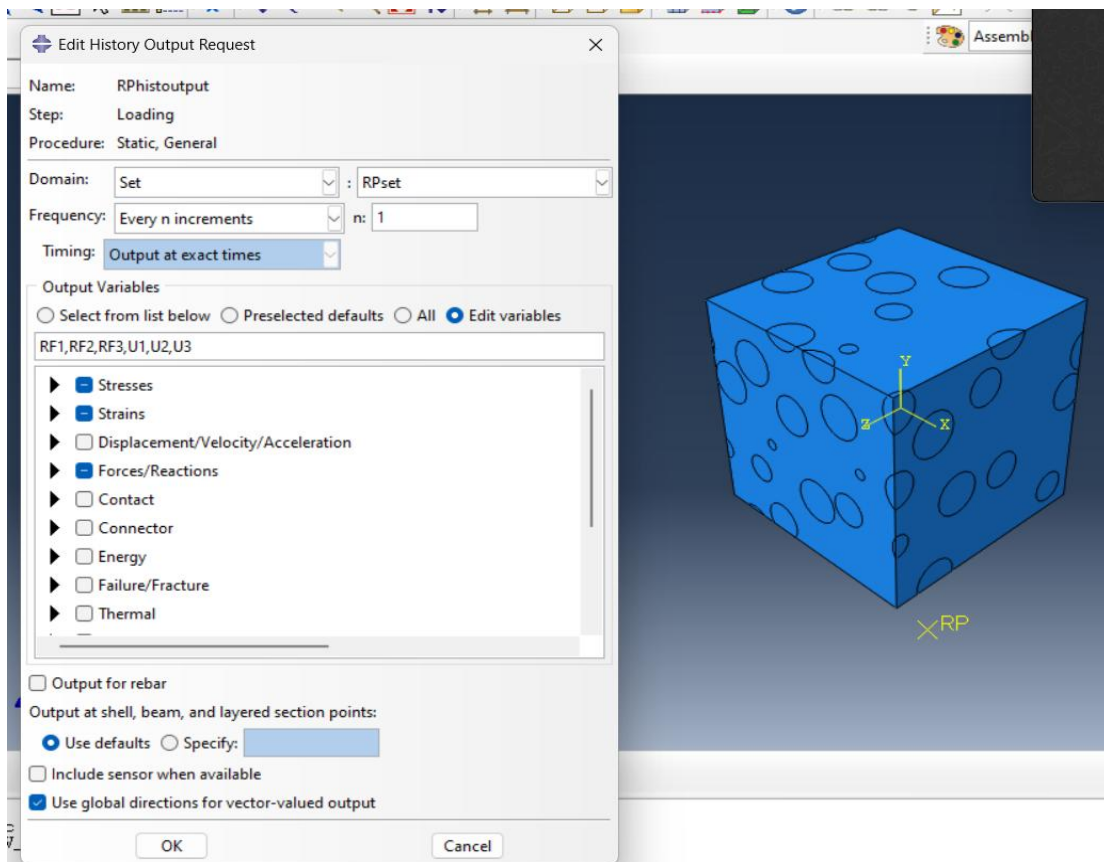
Step 6: Create a Reference Point and create a set for reference point in the assembly:



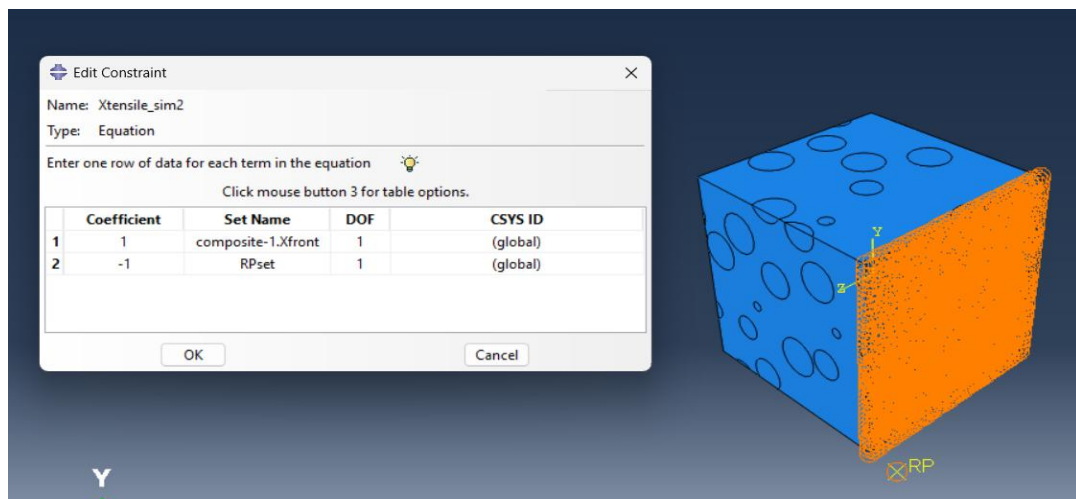
Step 7: Create a Loading Step:



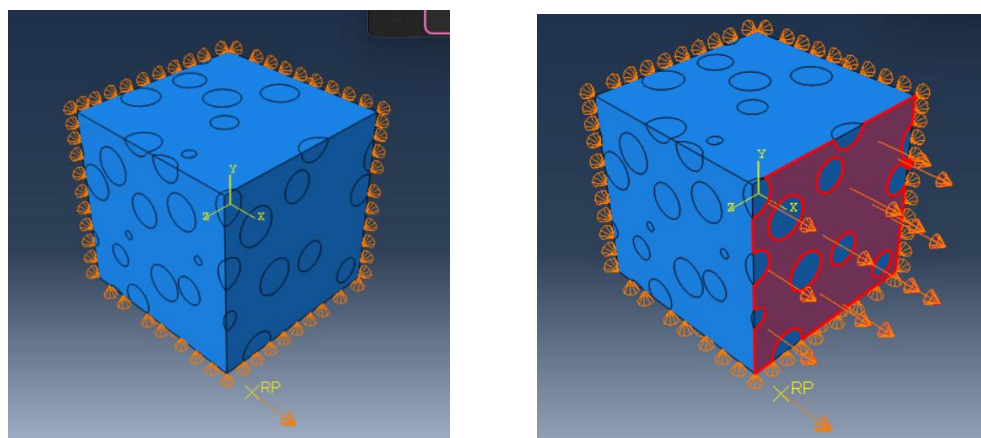
Step 8: Create History Output and Select the output variables



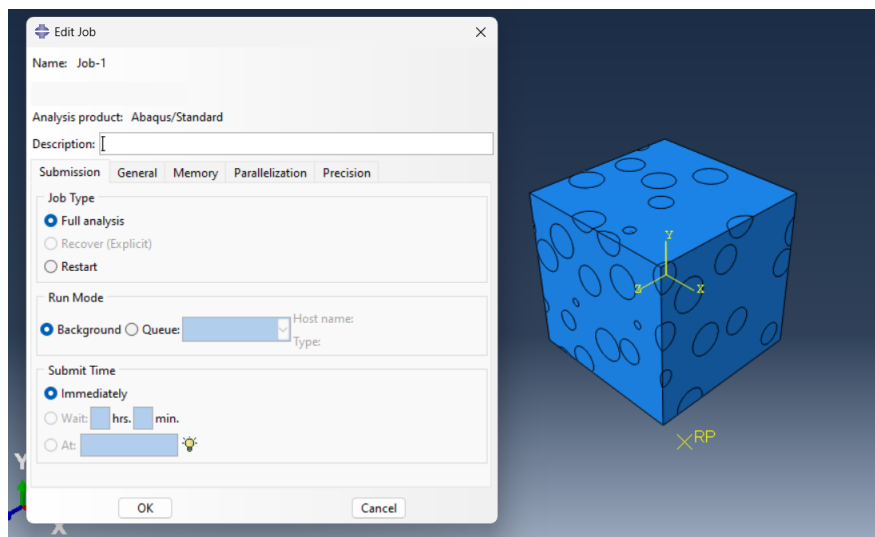
Step 9: Create constraints on the side on which the load is supposed to be applied:



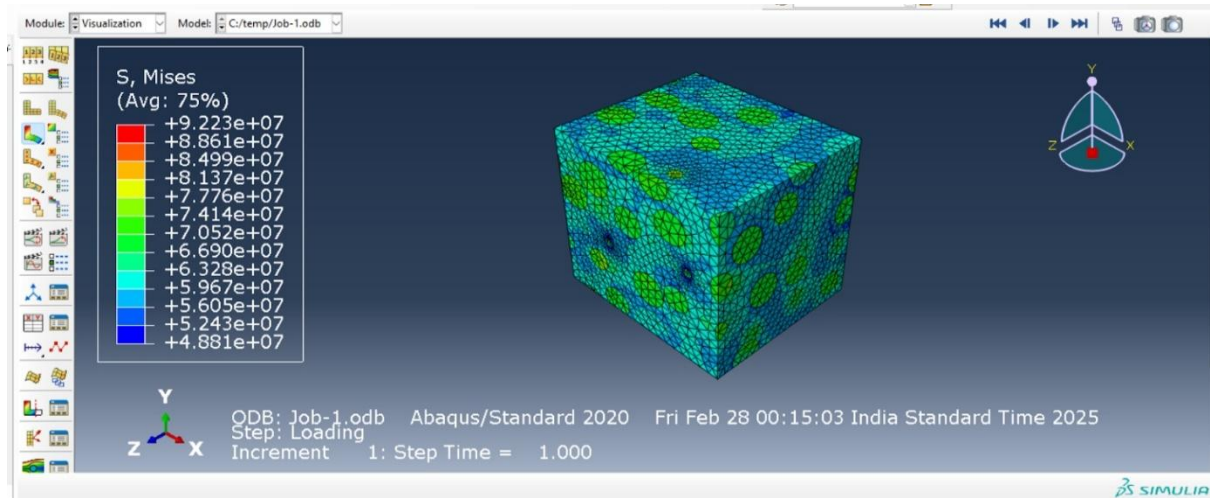
Step 10: Fix all the bases through boundary conditions and apply the Load: Load is applied in the form of pressure and then the load applied is -100Mpa.



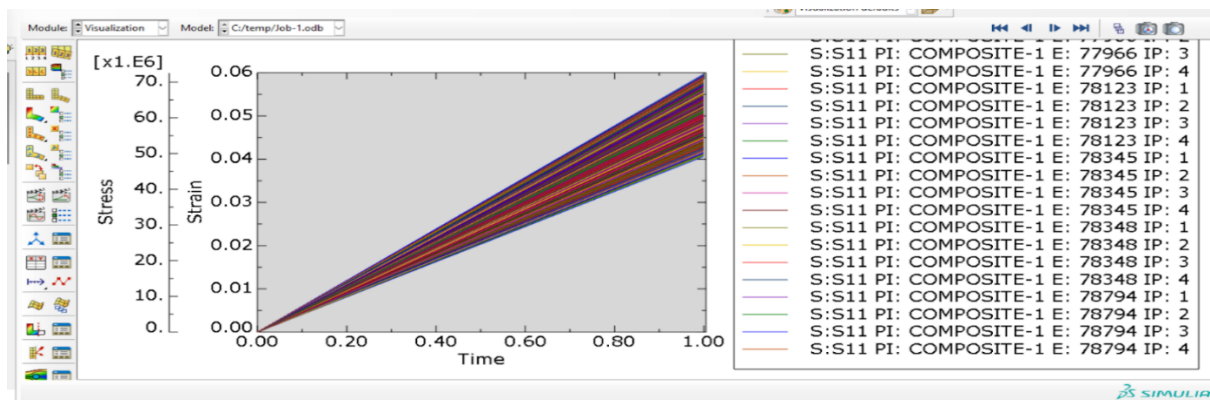
Step 11: Create Job and Submit:



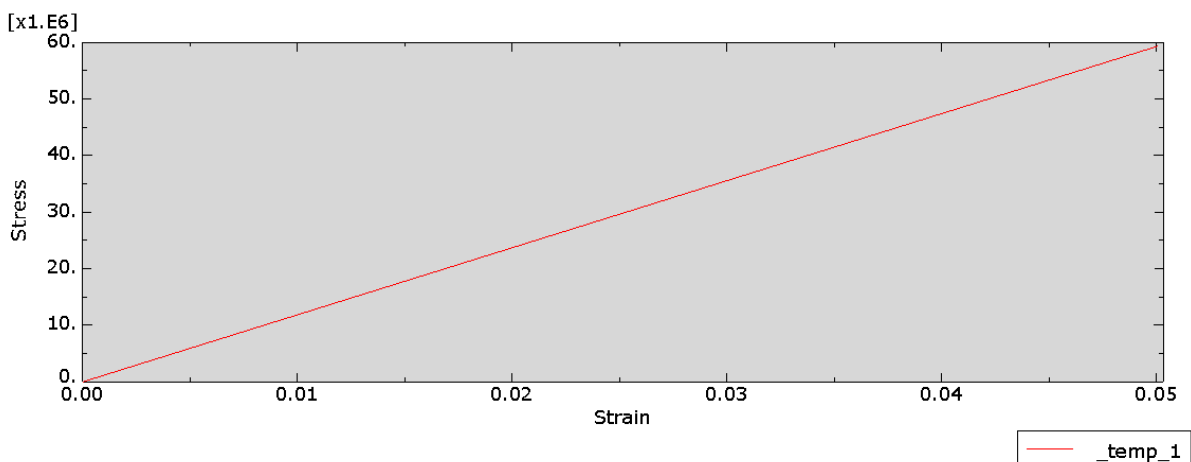
Step 12: Visualization:



Step 13: The output variables: Stress- Strain of the selected side (all elements) are plotted w.r.t time.



To get the final value, the ‘combine’ function in operate on XY data. The graph for stress strain of each element can be plotted as shown:



To get the average value of all elements, use the average function and export into excel to find the average modulus value of composite. The sand property value for which the value obtained closer to the experimental value is considered.

4.4 Rule of Mixtures

We used the **Rule of Mixtures** to calculate the theoretical modulus of sand. The formula for the composite modulus is: $E_c = V_f E_f + V_m E_m$

where Ec is the modulus of the composite, Ef is the modulus of sand, Em is the modulus of epoxy, and Vf andVm are the volume fractions of sand and epoxy, respectively.

Rearranging to solve for Esand:

$$E_{\text{sand}} = \frac{E_c - V_m E_{\text{epoxy}}}{V_f}$$

By substituting the given values, we determined the theoretical modulus of sand required to achieve the target composite modulus.

5. Results

1. Displacement Boundary Condition

Size of sand	Volume fraction	E_sand extracted from DIGIMAT
0.3	0.2	1.32E+09
	0.3	2.29E+09
	0.4	2.54E+09
	0.6	2.81E+09
	0.7	3.33E+09
0.425	0.2	1.33E+09
	0.3	1.68E+09
	0.4	1.60E+09
	0.5	1.63E+09
	0.6	1.77E+09

2. Periodic Boundary Condition

Size of sand	Volume fraction	E_Sand extracted from DIGIMAT
0.3	0.2	1.29E+09
	0.3	2.30E+09
	0.4	2.63E+09
	0.6	4.08E+09
	0.7	4.75E+09
0.425	0.2	1.33E+09
	0.3	1.68E+09
	0.4	1.69E+09
	0.5	1.65E+09
	0.6	1.83E+09

3. Uniaxial Stress Boundary Condition

Size of sand	Volume fraction	E_Sand extracted from ABAQUS
0.3	0.2	1.21E+09
	0.3	1.52E+09
	0.4	1.82E+09
	0.6	2.44E+09
	0.7	2.75E+09
0.425	0.2	1.25E+09
	0.3	1.50E+09
	0.4	1.75E+09
	0.5	2.0E+09
	0.6	2.25E+09

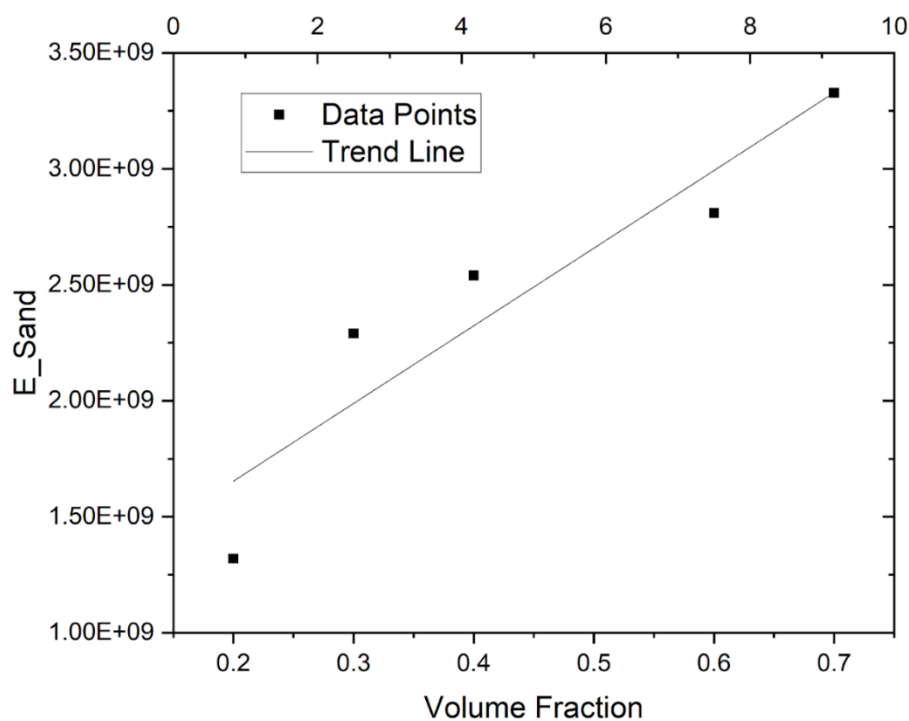
4. Rule of Mixtures

Size of sand	Volume fraction	E_Sand extracted from ABAQUS
0.3	0.2	1.30E+09
	0.3	2.07E+09
	0.4	2.22E+09
	0.6	1.97E+09
	0.7	2.08E+09
0.425	0.2	1.33E+09
	0.3	1.63E+09
	0.4	1.57E+09
	0.5	1.58E+09
	0.6	1.64E+09

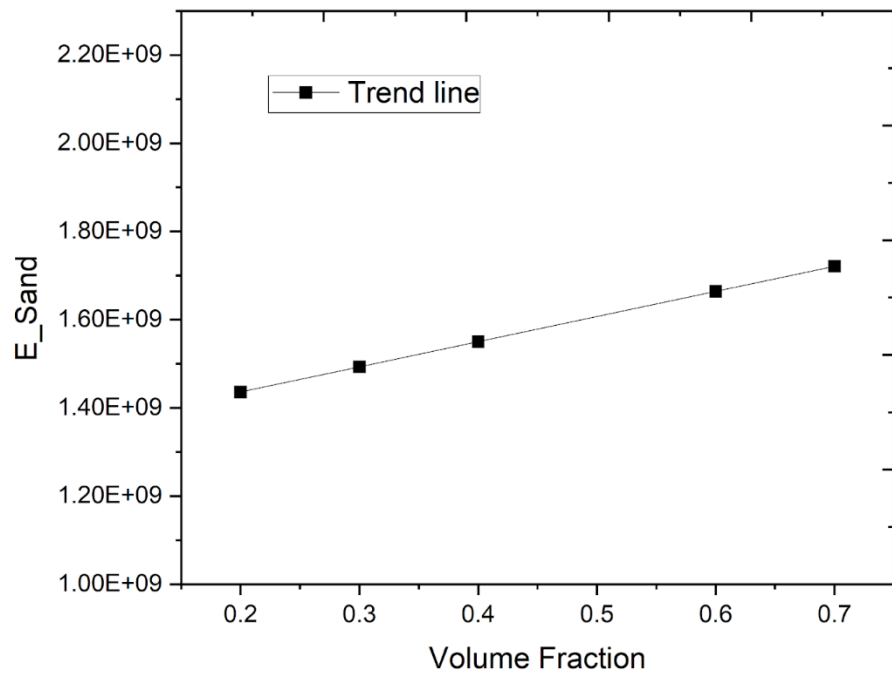
Graphs:

1. Displacement Boundary Condition Graphs:

(i) 0.3mm sand size

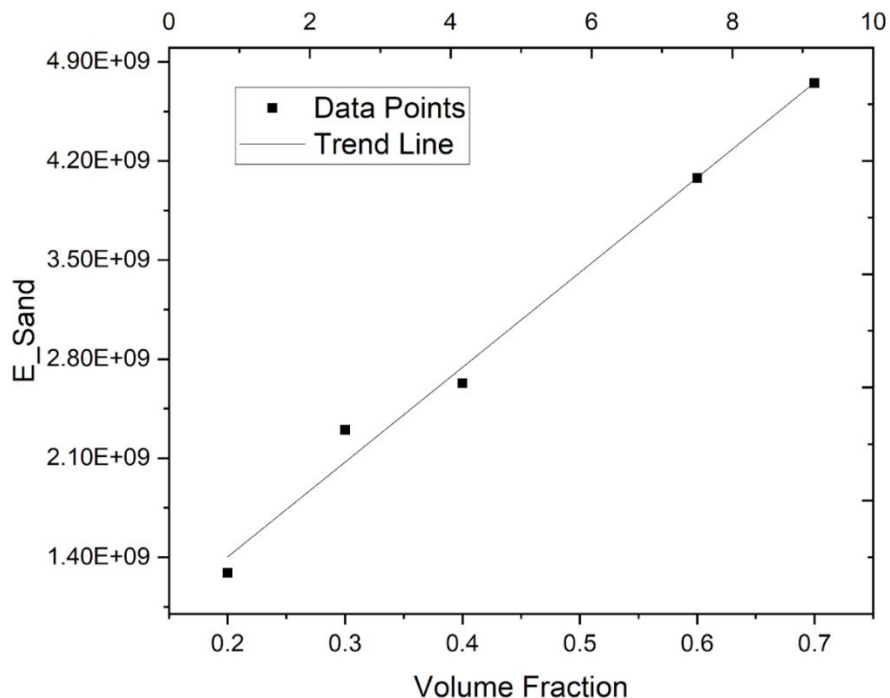


(ii) 0.425mm size

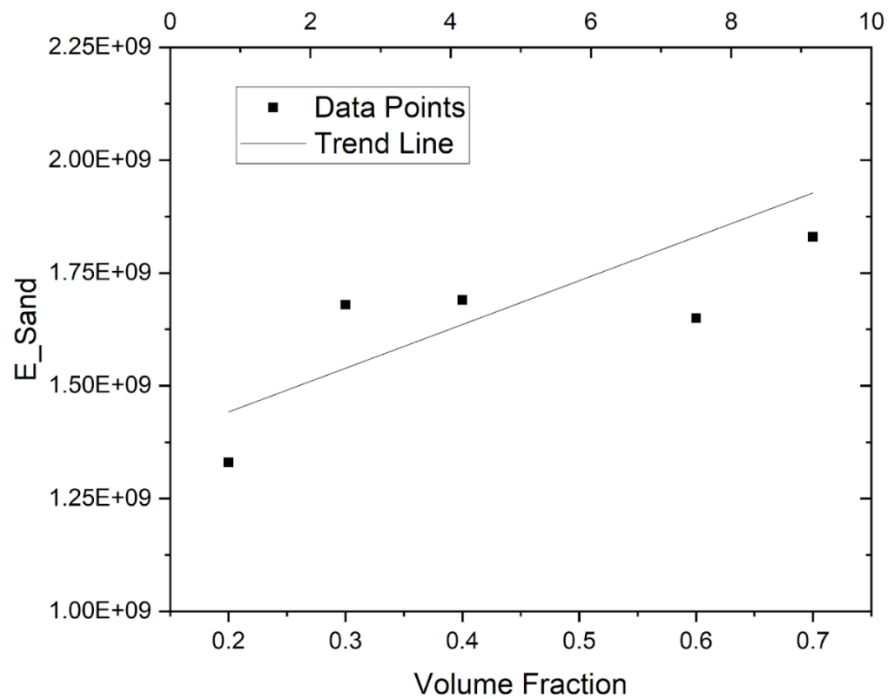


2. Periodic Boundary Condition

(i) 0.3mm size

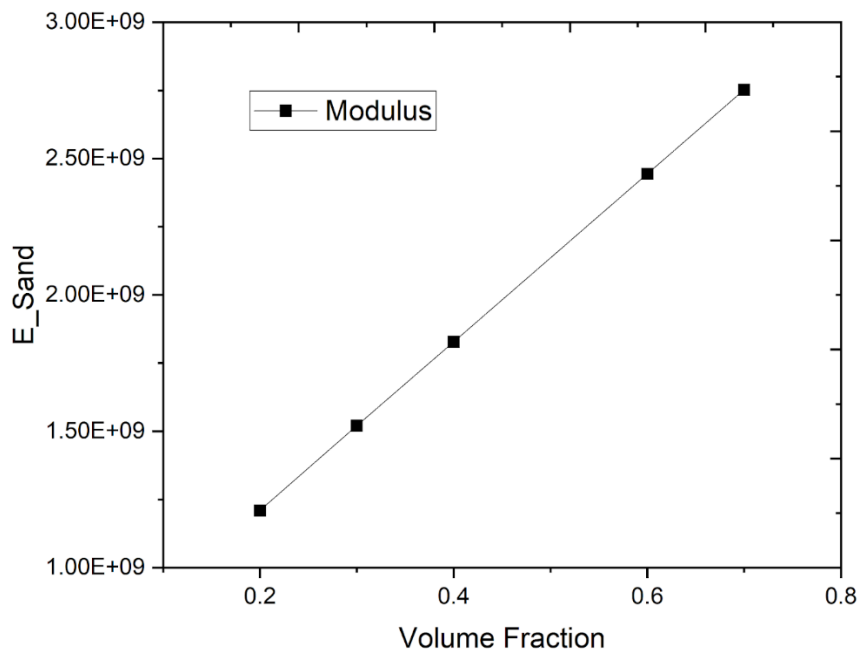


(ii) 0.425mm size

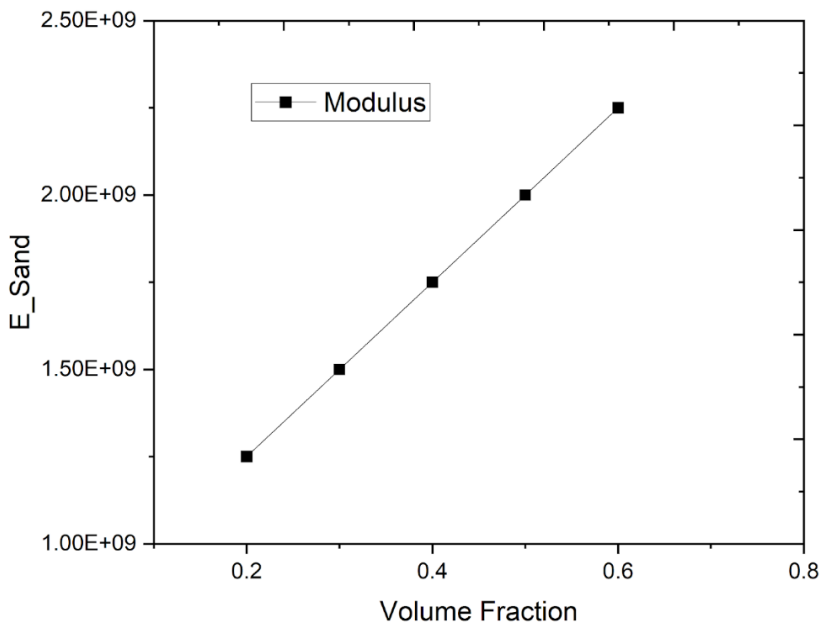


5. Uniaxial Stress Boundary Condition

(i) 0.3mm



(ii) 0.425 mm



6. Sieve Analysis

The sieve analysis was conducted on four different sand samples, each with distinct average particle sizes: **0.150 mm**, **0.300 mm**, **0.425 mm**, and **0.600 mm**. The corresponding particle size distribution graphs show fairly narrow spreads, indicating that the materials are **uniformly graded**, with particle sizes concentrated around their respective means.

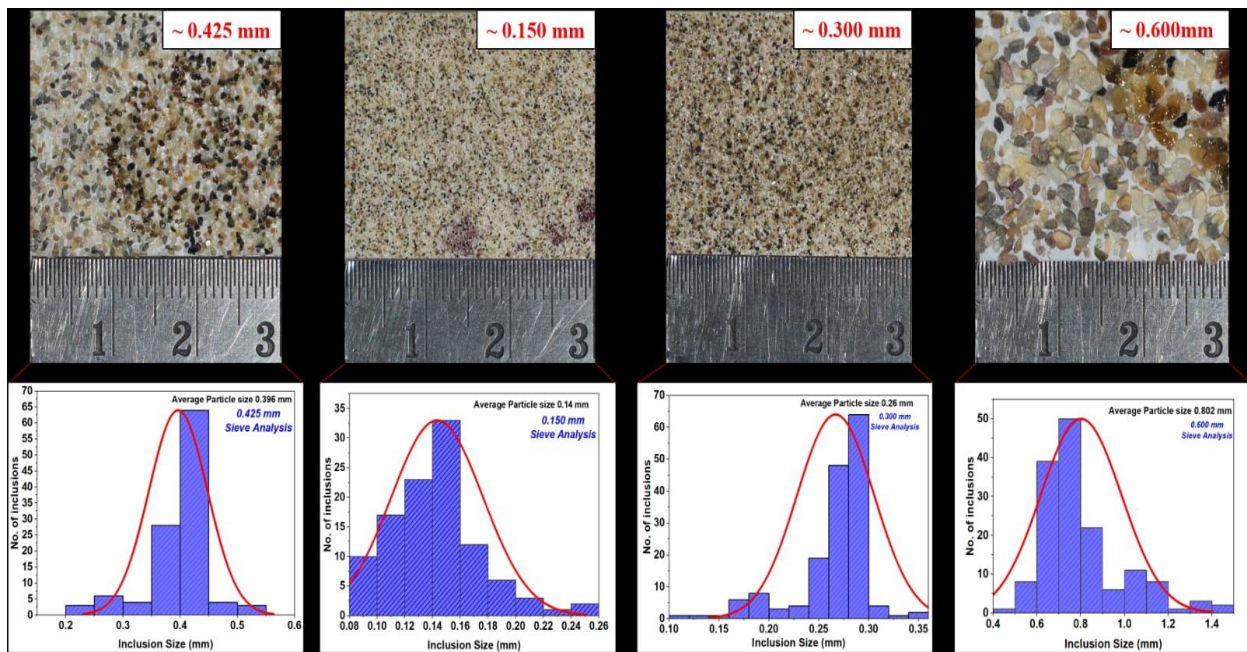


Fig. Sieve Distribution Graphs

Key Observations:

Sample 1 (0.150 mm): Very fine sand. The average particle size: **0.14 mm**. The steep distribution curve indicates uniformity in particle size.

Sample 2 (0.300 mm): Medium-fine sand. The average particle size: **0.26 mm**. The narrow distribution suggests uniform gradation.

Sample 3 (0.425 mm): Medium sand. The average particle size: **0.396 mm**. It is a well-distributed but still relatively uniform.

Sample 4 (0.600 mm): Coarse sand or fine gravel. The average particle size: **0.802 mm**. There is broader distribution but is still skewed towards uniformity.

So, from this we can understand that there is a uniform distribution of sand.

7. Contact Angle

We tested 3 different epoxy's on sand particles to find the contact angle.



LY556 Epoxy:

Epoxy Type	Inclusion	Sample Number	Contact Angle (T1)	Contact Angle (T2)	Contact Angle (T3)
LY	150 - Sand	1	81.521	59.27	44.145
		2	79.067	57.427	51.481
		3	81.008	63.45	38.494
LY	300- Sand	1	85.438	55.95	50.512
		2	84.646	66.258	46.436
		3	81.347	55.796	41.126
LY	425- Sand	1	74.663	44.147	32.918
		2	71.565	47.662	42.623
		3	70.309	36.977	42.648

LY	600- Sand	1	81.557	74.055	60.072
		2	68.916	61.19	56.505
		3	73.803	69.986	60.791

ER099 Epoxy:

Epoxy	Sample	Contact Angle (T1)	Contact Angle (T2)	Contact Angle (T3)
ER	150	62.367	33.69	21.089
		60.764	36.816	17.582
		64.67	32.266	29.957
ER	300	51.892	33.394	29.867
		47.426	30.167	22.687
		53.079	30.099	20.247
ER	425	41.836	32.471	-
		36.634	20.127	-
		45	25	-
ER	600	53.011	32.245	16.891
		45.163	29.56	17.051
		72.626	58.496	43.98

YDL Epoxy:

Epoxy	Inclusion	Sample Number	Contact Angle (T1)	Contact Angle (T2)	Contact Angle (T3)
YDL	150	1	50.746	26.9	17.301
		2	76.305	41.084	22.586
		3	72.28	37.225	25.671
YDL	300	1	50.663	35.121	-
		2	48.215	29.874	-
		3	53.715	34.026	-
YDL	425	1	62.158	27.85	17.816

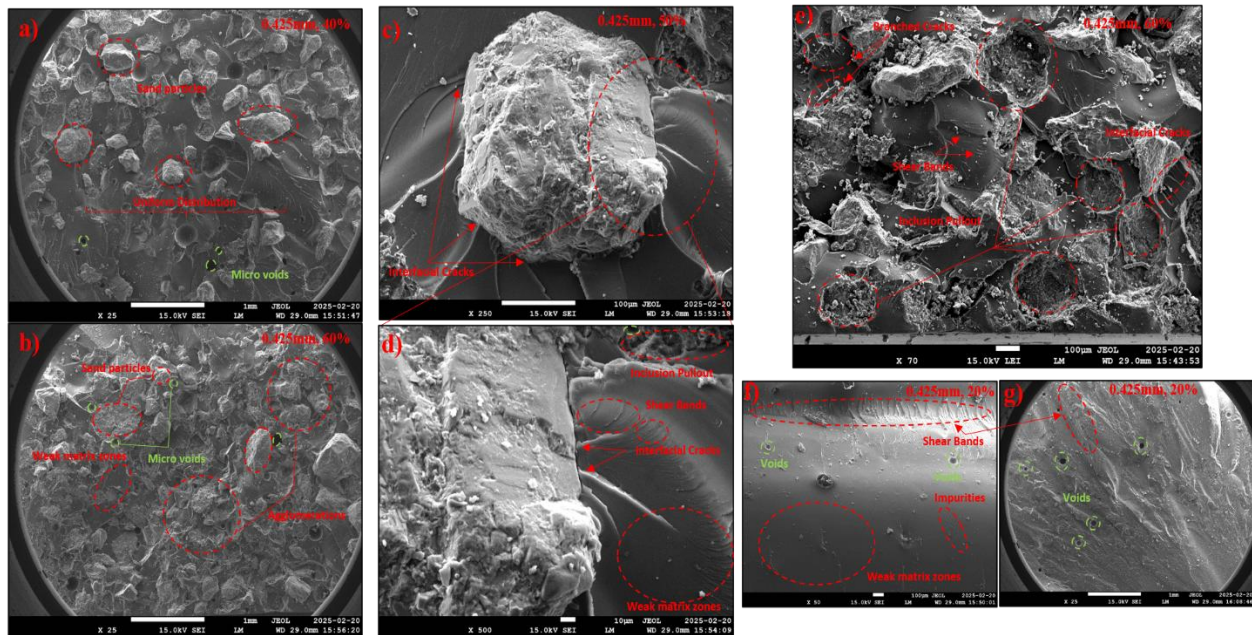
		2	43.543	17.396	15.832
		3	63.892	36.417	25.981

Material / Epoxy	Epoxy -01 (ER)			Epoxy – 02 (LY)			Epoxy – 03 (YDL)		
	T1	T2	T3	T1	T2	T3	T1	T2	T3
Sand - 150 micrometres									
Sand – 300 micrometres									
Sand – 425 micrometres									
Sand – 600 micrometres									

8. SEM Analysis

To analyze post-failure microstructure of samples composed of sand particles of two size ranges, 425 μm and 300–600 μm , after tensile loading SEM analysis was performed. The goal is to observe failure mechanisms, fracture features, and interfacial behavior.

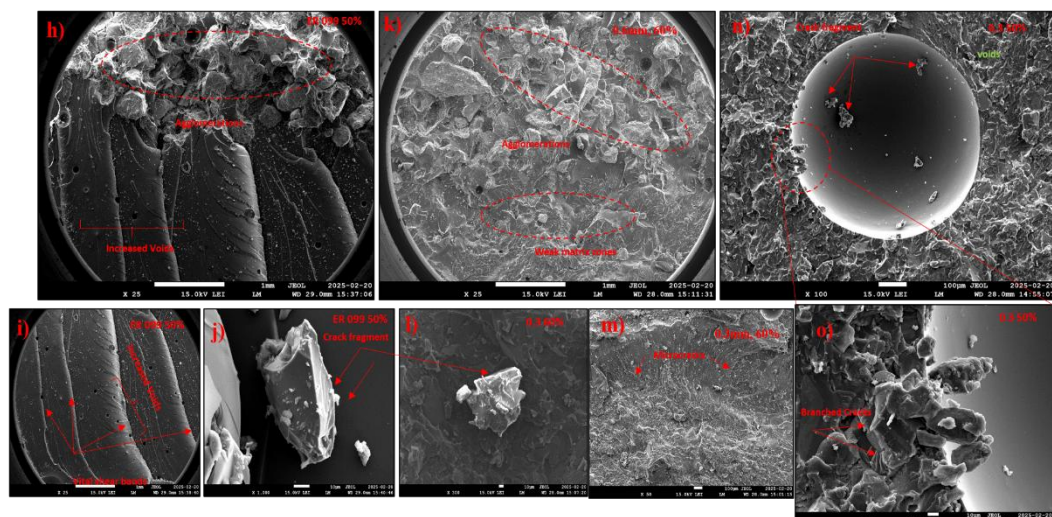
I. 425 μm Sand – Post-Tensile Test SEM Observations



Fracture Behavior, Brittle Failure Dominance: Multiple fractured edges, sharp cracks, and angular particle breakage. **Shear Bands & Crack Initiation Zones:** Indicate localized plastic deformation before failure. Cracks propagate along weak interface zones.

Surface Morphology: Microvoids and Intergranular Fractures: Suggest weak particle-matrix bonding or inter-particle cohesion. Debonding appears to initiate at interfaces under tensile strain.

II. 300–600 μm Sand – Post-Tensile Test SEM Observations



Fracture Behavior Brittle fracture is still present, but there's more evidence of ductility and thermal softening. **Crack Coalescence and Pull-out:** Crack fragments, larger interfacial cracks, and signs of particle dislodgement suggest better energy absorption before failure.

Surface Morphology: Larger voids and smoother fracture planes than in 425 μm samples. Presence of eutectic-like structures in some cases.

Feature	425 μm Sand	300–600 μm Sand
Fracture Mode	Primarily brittle	Mixed brittle/ductile with thermal influences
Void Formation	Microvoids, early debonding	Larger, evolved voids and crack coalescence
Particle-Matrix Interface	Weak bonding, early crack initiation	Slightly better bonding, delayed failure
Thermal Influence	None / minimal	Evident (spherical voids, melt regions)
Energy Absorption	Lower, fast crack propagation	Higher, more complex failure path

9. 3 Point Bending Test

To investigate the flexural behavior of our functionally graded material (FGM) specimens, we conducted both - a three-point bending test experimental test and a simulation using ABAQUS. This test was chosen to evaluate how the gradual variation in sand filler content across the thickness of the epoxy matrix affects the overall bending performance. Functionally graded materials exhibit continuous variation in mechanical properties, and the three-point bending setup is particularly effective in revealing how such gradation influences stress distribution and deflection under load. The ASTM standard chosen for our samples was ASTM D7264M.

The different combinations of FGM's we made were:

Sample Number	Sample Composition
1	300 : (60,50,40,30)
2	425 : (60,50,40,30)
3	(600-50% , 425-40%, 425-30%, 300-30%)
4	(300-40%, 600-50%, 600-50%, 300-40%)
5	(300-30%, 425-40%, 600-50%, 600-50%)

Sample 3: Gradual Hardening from Top to Bottom (High Resistance at Impact Face)

Layer 1 (top): 600 µm, 50% sand → Tough and stiff

Layer 2: 425 µm, 40% sand → Moderately tough

Layer 3: 425 µm, 30% sand → Slightly softer

Layer 4 (bottom): 300 µm, 30% sand → Most compliant (good for energy dispersion)

Sample 4: Symmetric Structure for Balanced Behavior

Layer 1: 300 µm, 40%, Layer 2: 600 µm, 50%

Layer 3: 600 µm, 50% , Layer 4: 300 µm, 40%

This offers good stiffness in the center with softer outer layers to reduce cracking

Sample 5: Toughness Gradient (Soft to Hard). To absorb energy gradually:

Layer 1 (top): 300 µm, 30%

Layer 2: 425 µm, 40%

Layer 3: 600 µm, 50%

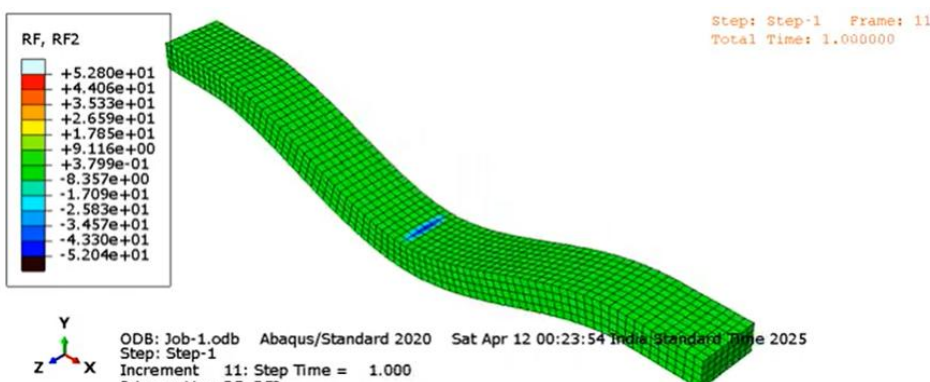
Layer 4 (bottom): 600 µm, 50%

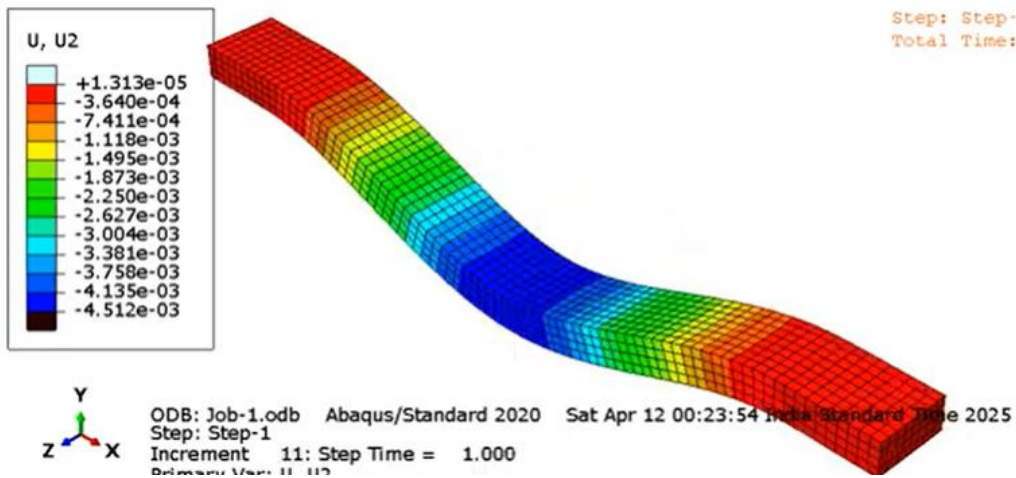
This approach minimizes stress concentrations and spreads out the energy.

9.1 ABAQUS Simulation of 3 point bending test for FGM

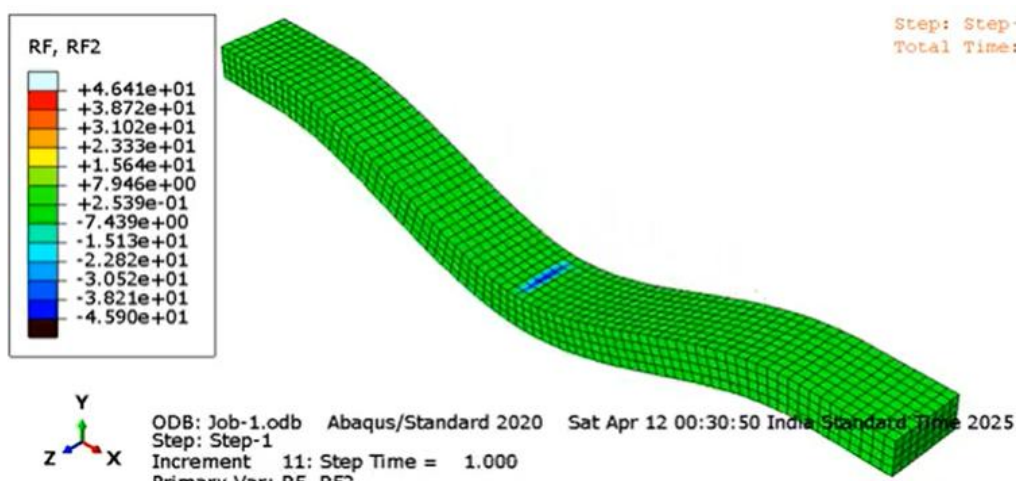
We modeled the FGM specimen in ABAQUS, assigning different material properties to layers. Appropriate boundary conditions were applied: supports at two ends and a centrally applied load.

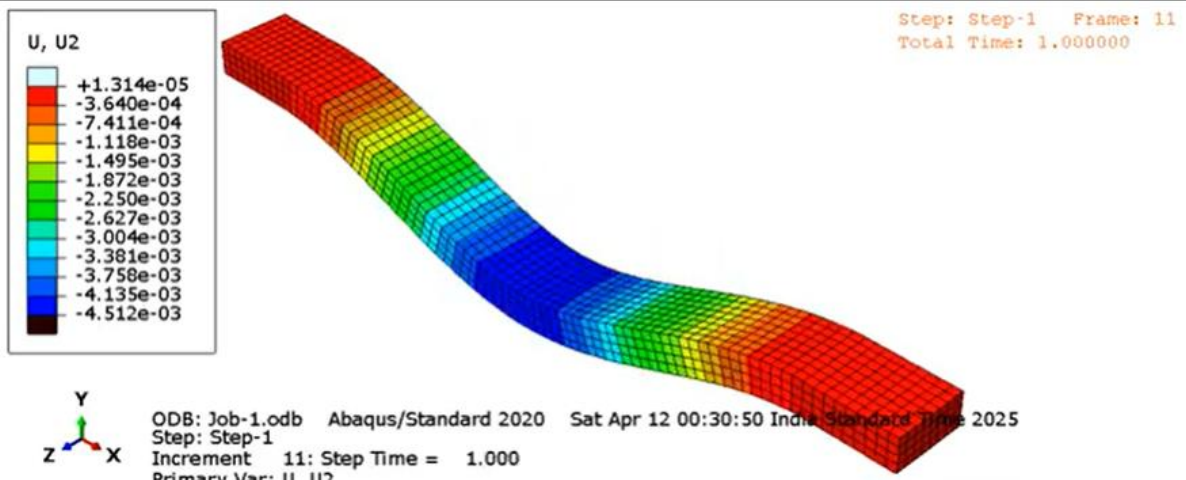
Sample 1:



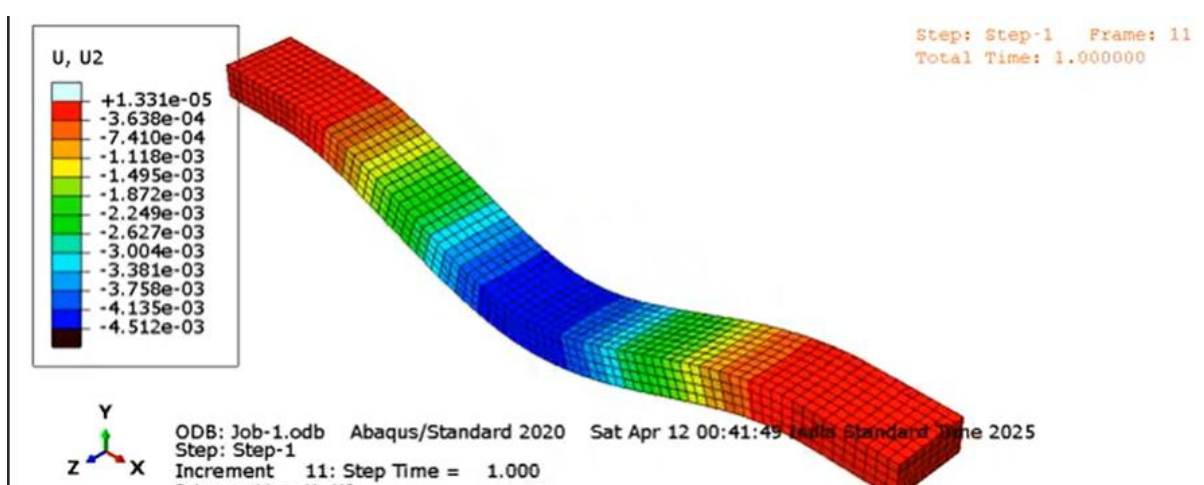
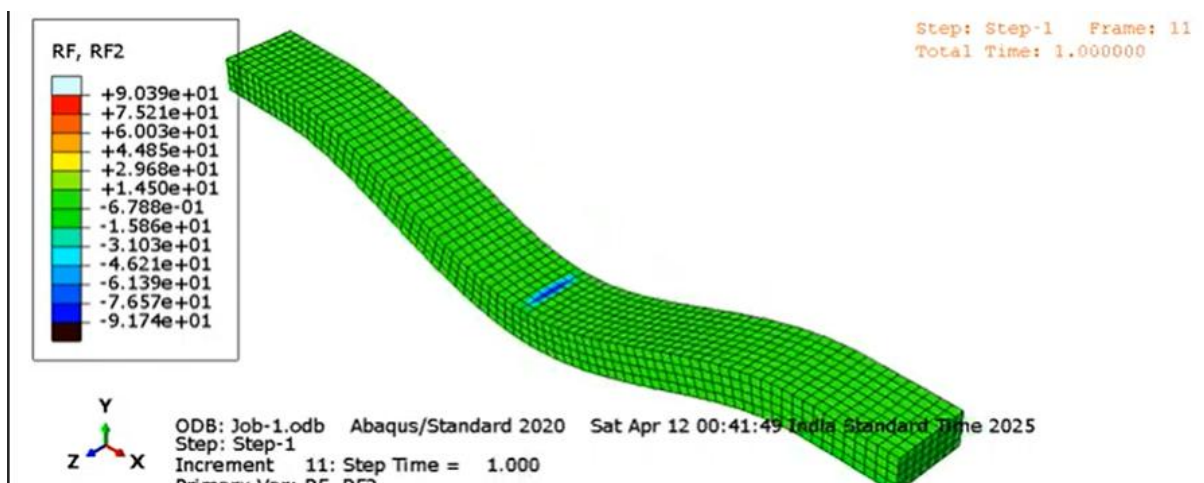


Sample 2:

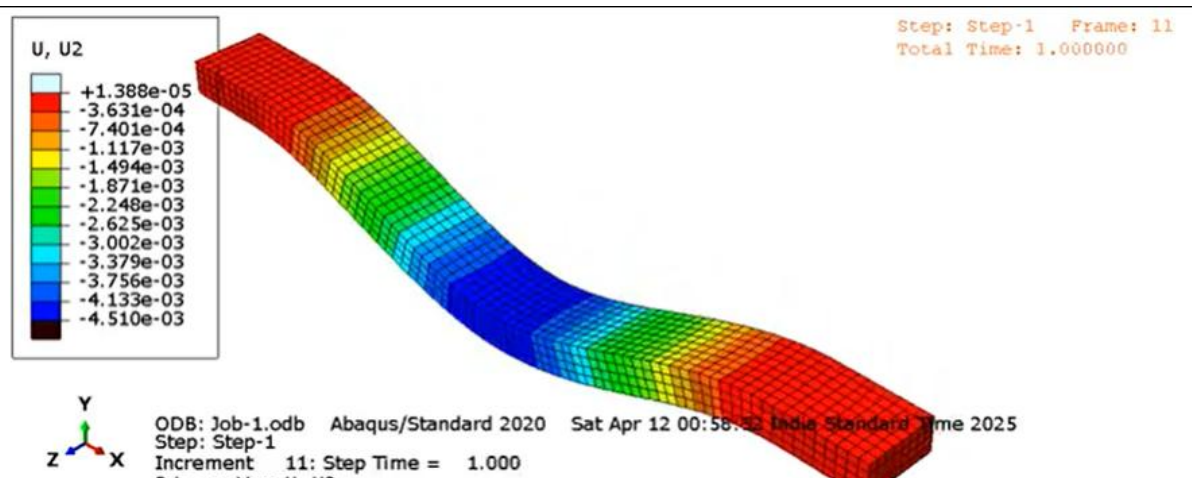
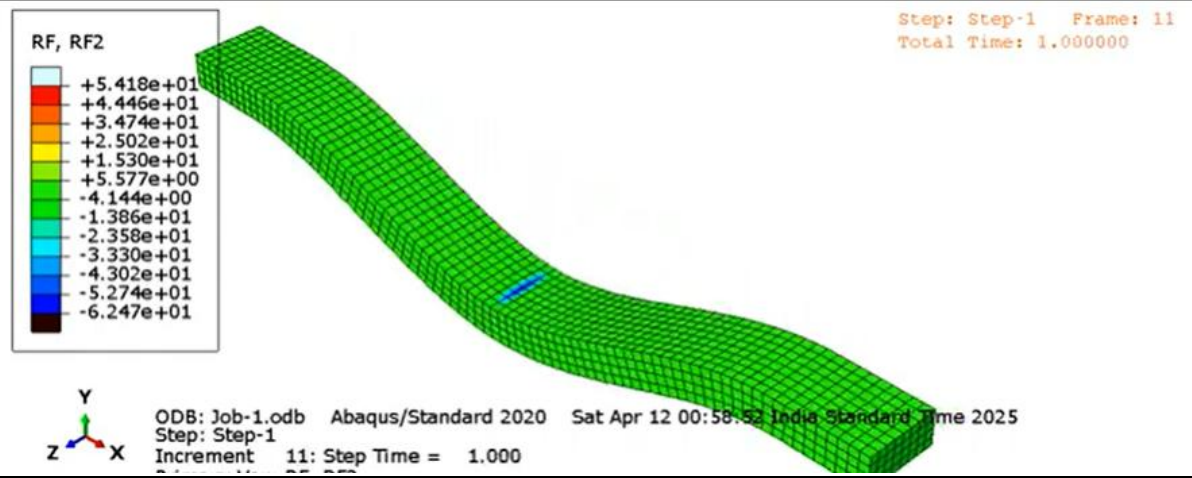




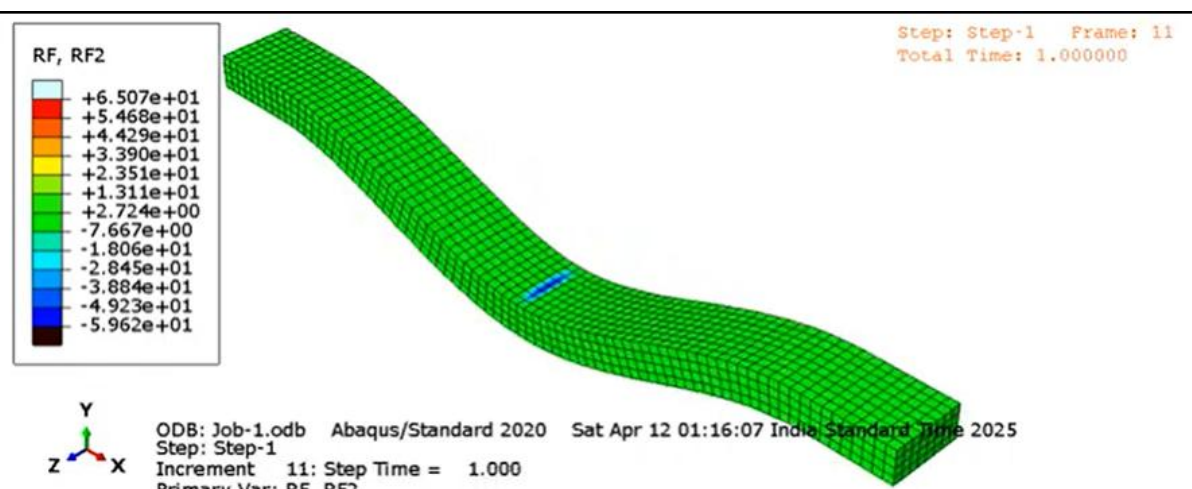
Sample 3:

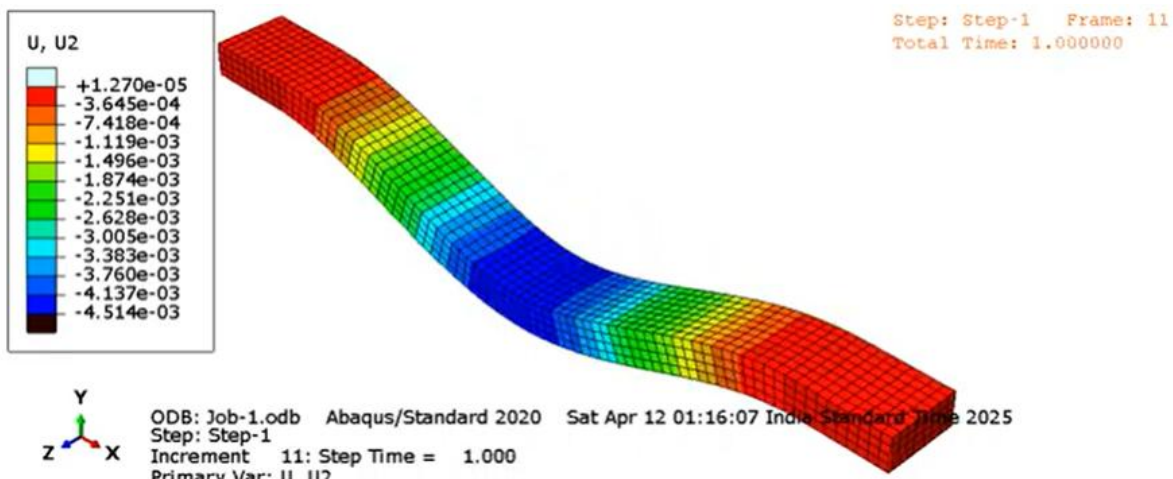


Sample 4:

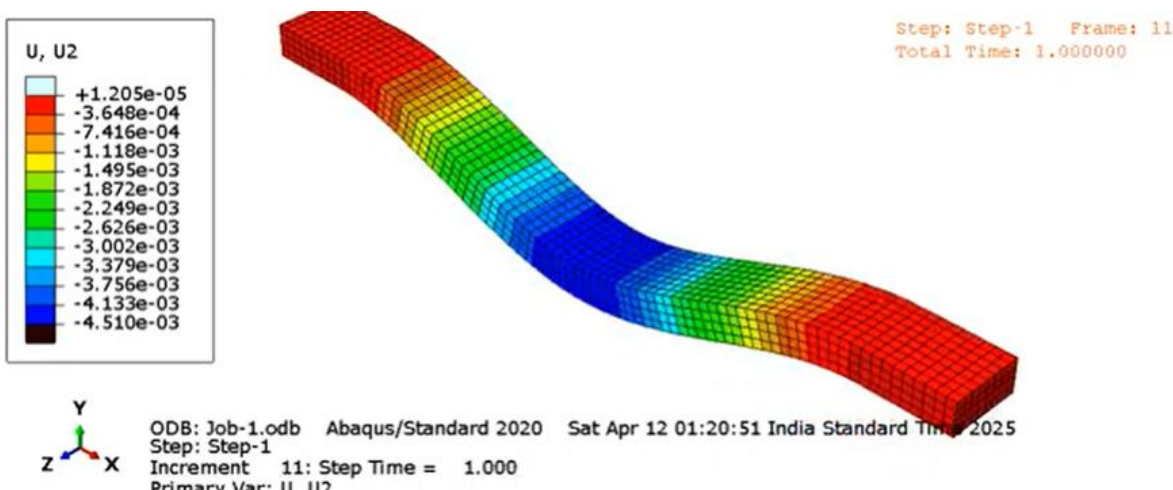
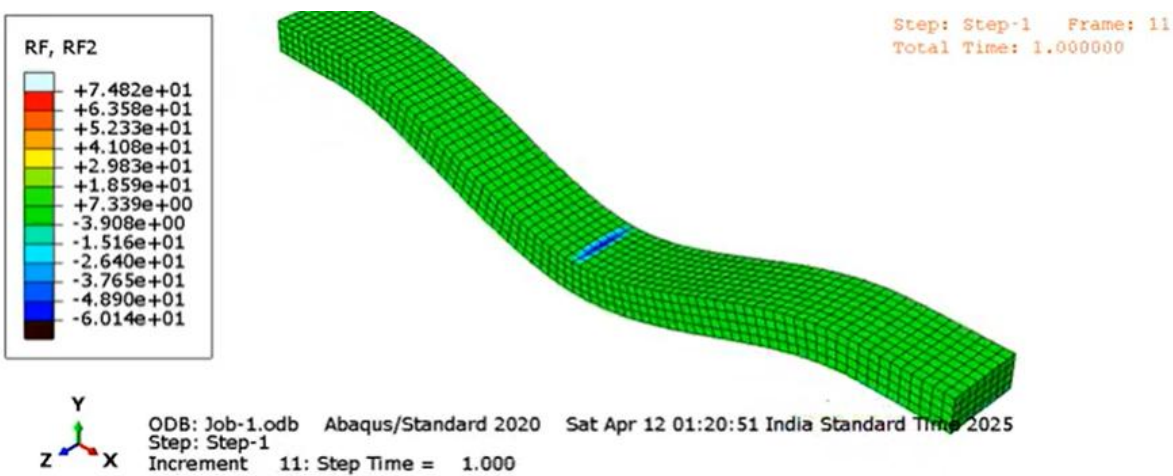


Sample 5:





Sample 6:



Result:

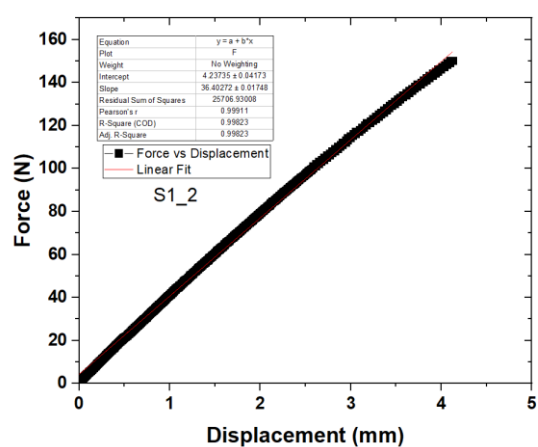
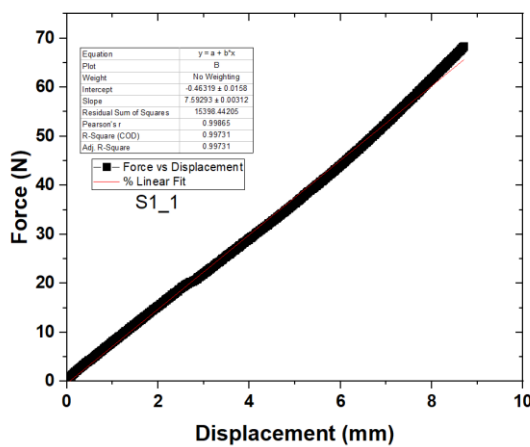
Sample Number	Sample Composition	Force (-Y direction)	Displacement (-Y direction) in mm	Flexural Stress (Pa)	Flexural Modulus	K	EI
1	300 : (60,50,40,30)	52.0397	4.5	9.75744375	936.4059154	11.56437778	0.0009868269037
2	425 : (60,50,40,30)	45.9007	4.5	8.60638125	825.9403302	10.20015556	0.0008704132741
3	(600-50% , 425-40%, 425-30%, 300-30%)	62.4651	4.5	11.71220625	1124.001275	13.88113333	0.001184523378
4	(300-40%, 600-50%, 600-50%, 300-40%)	59.6222	4.5	11.1791625	1072.845938	13.24937778	0.00113061357
5	(300-30%, 425-40%, 600-50%, 600-50%)	60.1447	4.5	11.27713125	1082.247839	13.36548889	0.001140521719

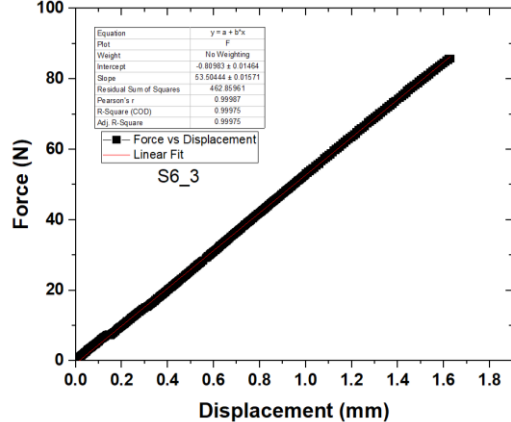
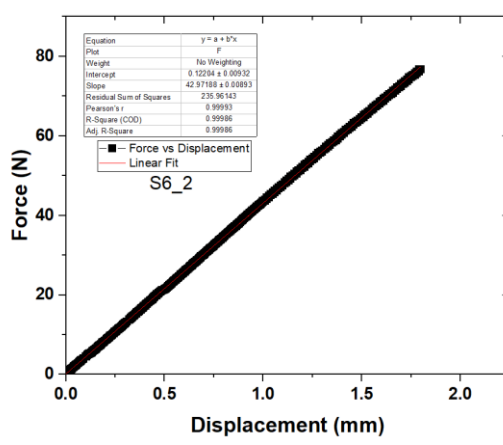
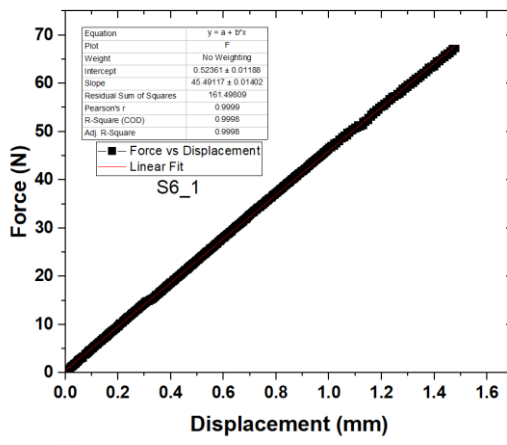
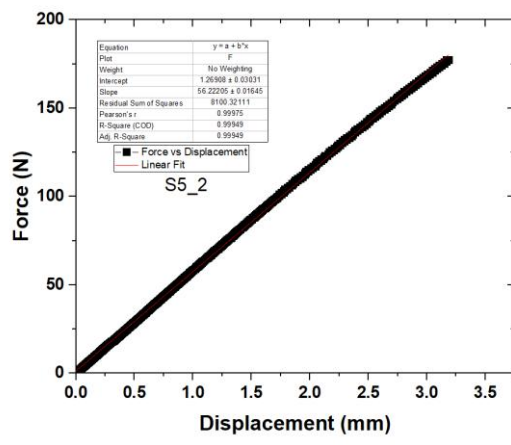
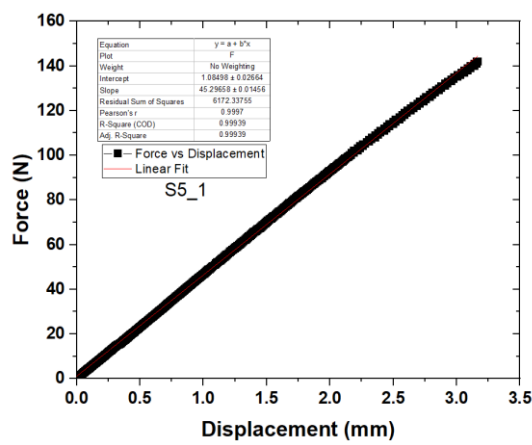
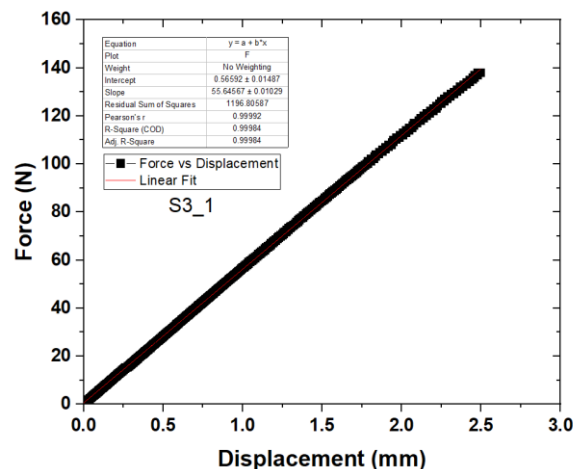
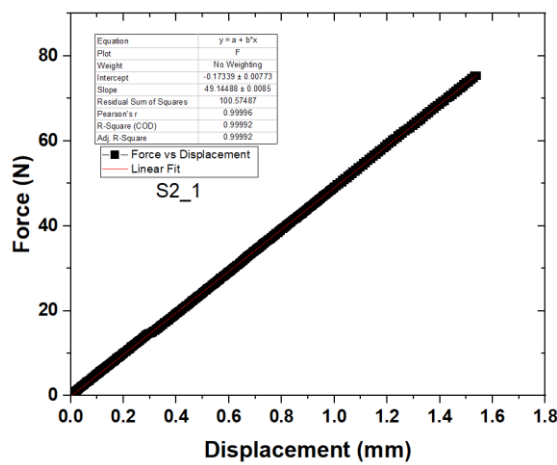
9.2 Experimental 3 point bending test for FGM



Fig. Flexural Samples

Result Graphs: The sample wise Force vs Displacement graphs are as follows





Sample No.	Average K (N/mm)	Average EI (N·mm ²)
1	21.99783	0.00187715
2	49.14488	0.00419370
3	55.64567	0.00474843
4	50.75932	0.00433146
5	47.32250	0.00403818

Inference from experimental and simulation:

From the comparison between the simulation and experimental results of the three-point bending test for Functionally Graded Materials (FGMs), it can be observed that:

1. Flexural Modulus (EI) and Stiffness (K) values obtained from simulation are slightly lower than those obtained experimentally across all sample compositions.
2. Despite the difference in magnitude, the trend across different samples remains consistent, indicating that simulation can still effectively capture the relative mechanical performance between different gradient compositions.
3. The sample with the most complex gradient (Sample 3) shows the highest flexural performance in both simulation and experiment. This gradation from **stiff to soft layers** optimizes stress distribution and helps delay crack propagation, thereby improving both **flexural performance and impact resistance**.

Overall based on this we can fine tune our sample configurations of FGMs based on requirements.

10. Conclusion

In conclusion, the project on the development of sand composites for high-impact resistance has successfully demonstrated the potential of sand-reinforced epoxy composites as a cost-effective and sustainable solution for ballistic protection. Through a combination of experimental work and computational modeling, we have shown that incorporating sand particles into epoxy significantly enhances the material's hardness, impact resistance, and energy dissipation, making it a promising candidate for protective applications. The impact resistance of the composite was one of the key areas of focus in this project. We observed that increasing the sand volume fraction led to a substantial improvement in the composite's ability to withstand high-velocity impacts. The sand particles contributed to better energy absorption and distribution, reducing the extent of damage upon impact. Although challenges such as material uniformity and bonding strength were encountered, they were addressed through a detailed analysis of the composite's microstructure and performance under high-impact conditions. The results of the impact tests validated the effectiveness of sand composites in absorbing and dissipating impact energy, a crucial factor in designing materials for ballistic applications. Our study also clearly demonstrates that using Functionally Graded Materials (FGMs) significantly improves the flexural performance of epoxy–sand composites. By strategically varying sand particle size and concentration across layers, particularly in a top-to-bottom hard-to-soft configuration, FGMs help achieve better stress distribution and energy absorption. Among all configurations, Sample 3, which used a graded structure from 600 μm –50% at the impact face to 300 μm –30% at the bottom, showed the highest values of stiffness (K) and flexural rigidity (EI) in both experimental and simulation results. This confirms that FGMs are more effective than homogeneous or non-graded composites. Our research lays the groundwork for further refinement in manufacturing processes and material optimization.

11. References

1. [https://www.researchgate.net/publication/283338557 Development of RVE-embedded solid elements model for predicting effective elastic constants of discontinuous fiber reinforced composites](https://www.researchgate.net/publication/283338557)
2. [Numerical modelling of flax short fibre reinforced and flax fibre fabric reinforced polymer composites - ScienceDirect](#)
3. [Micro-mechanical analysis on random RVE size and shape in multiscale finite element modelling of unidirectional FRP composites - ScienceDirect](#)
4. [RVE modelling of short fiber reinforced thermoplastics with discrete fiber orientation and fiber length distribution | Discover Applied Sciences](#)
5. <https://www.sciencedirect.com/science/article/pii/S0266353824005232>
6. https://www.tandfonline.com/doi/pdf/10.1080/1023666X.2022.2164826?casa_token=KAzDcyxvddcAAAAA:EJTWOy5E91D5vx3pJnwyCTFuQQEHDjdHph9iTOHLoMLOVnBjyLMZPeZEyKYoNIlleUBXtv4sl03Lks
7. <https://journals.sagepub.com/doi/full/10.1177/15280837211000365>
8. https://www.sciencedirect.com/science/article/abs/pii/S0300944022004490?fr=RR-2&ref=pdf_download&rr=93ecf77068a279da
9. https://acsess.onlinelibrary.wiley.com/doi/abs/10.2136/sssaj2000.642564x?casa_token=l7f5xu8JuKOAAAAA%3A-ak495_sQpTCEEcFbfPhMWk6lubkpVmX2Wqlxr1gaxhClAz2b5pMfxfBSCyl2NK3LBu6TItQtQq-ko
10. <https://onlinelibrary.wiley.com/doi/abs/10.1002/esp.3290130609>
11. <https://onlinelibrary.wiley.com/doi/epdf/10.1002/jcb.5000650902>